Probing Molecular Interactions within Class II MHC A^q/Glycopeptide/T-Cell Receptor Complexes Associated with Collagen-Induced Arthritis

Ida E. Andersson,[†] Balik Dzhambazov,[‡] Rikard Holmdahl,[‡] Anna Linusson,*[,†] and Jan Kihlberg*[,†,§]

Department of Chemistry, Umeå University, SE-901 87 Umeå, Sweden, Medical Inflammation Research, BMC I11, Lund University, SE-221 84 Lund, Sweden, and AstraZeneca R&D Mölndal, SE-431 83 Mölndal, Sweden

Received May 9, 2007

T cells obtained in a mouse model for rheumatoid arthritis are activated by a glycopeptide fragment from rat type II collagen (CII) bound to the class II major histocompatibility complex A^q molecule. We report a comparative model of A^q in complex with the glycopeptide CII260-267. This model was used in a structure-based design approach where the amide bond between Ala^{261} and Gly^{262} in the glycopeptide was selected for replacement with ψ[COCH$_2$], ψ[CH$_2$NH$_2^+$], and ψ[(*E*)-CH═CH] isosteres. Ala-Gly isostere building blocks were then synthesized and introduced in CII260-267 and CII259−273 glycopeptides. The modified glycopeptides were evaluated for binding to the A^q molecule, and the results were interpreted in view of the A^q/glycopeptide model. Moreover, recognition by a panel of T-cell hybridomas revealed high sensitivity for the backbone modifications. These studies contribute to the understanding of the interactions in the ternary A^q/glycopeptide/T-cell receptor complexes that activate T cells in autoimmune arthritis and suggest possibilities for new vaccination approaches.

Introduction

Autoimmune diseases are characterized by the immune system responding to self-tissue antigens. In rheumatoid arthritis (RA[a]), this specifically leads to chronic inflammation of the peripheral cartilaginous joints, eventually resulting in degradation of joint cartilage, irreversible bone erosion, and severe joint deformation.[1] Susceptibility to RA has been strongly correlated with the class II major histocompatibility complex (MHC) genes HLA-DR4 and HLA-DR1, that code for the class II MHC molecules DR4 and DR1, respectively.[2−4] Class II MHC molecules are membrane-bound glycoproteins, with a molecular weight of approximately 60 kDa, that consist of two noncovalently associated chains, α and β.[5] These glycoproteins are found in antigen-presenting cells (APC), that is, macrophages, B cells and dendritic cells, where they bind peptide antigens obtained by degradation of extracellular proteins. The class II MHC molecule in complex with the peptide antigen is subsequently transported to the cell surface of the APC where it is presented for recognition by receptors on circulating CD4$^+$ T cells. Although the events initiating the immune response in RA are unknown, the specific inflammatory attack on joint cartilage indicates that T cells recognize a joint-specific self-antigen. Both T cells[6−8] and antibodies[9−11] directed against type II collagen (CII), which is the main protein in joint cartilage, have been found in RA patients, indicating that it is an important component of the disease pathology.

Collagen-induced arthritis (CIA) is an animal model for RA, where immunization of mice with CII derived from rat leads to similar symptoms and histopathology of the affected joints as seen in RA patients.[12] In a similar way that RA is associated with expression of DR4 and DR1, susceptibility to CIA in mice is genetically linked to the class II MHC A^q molecule.[13,14] It has been found that T cells obtained from mice with CIA are activated by the rat CII259−273 peptide sequence.[15] Further studies have revealed that Ile^{260} and Phe^{263} are critical residues for binding to A^q, while Lys^{264} is a major T-cell receptor (TCR) contact point.[16,17] Importantly, a majority of the T-cell hybridomas specifically recognize Lys^{264} when post-translationally hydroxylated and glycosylated with a β-D-galactopyranosyl residue (GalHyl^{264}).[18−20] This recognition is specific for individual hydroxyl groups on the carbohydrate moiety[15,21] and, in addition, also depends on interactions with the ϵ-amino group[19,22,23] in the hydroxylysine side chain and the *O*-glycosidic linkage.[22,24] The A^q binding preferences for some of the amino acid residues in CII260−267, which is the minimal epitope required for binding to A^q, while still being able to elicit a T-cell response,[25] have recently been described by a quantitative structure−activity relationship (QSAR) model.[26]

It has been shown that vaccination of mice with the CII259−273 glycopeptide in complex with soluble A^q protein can protect against CIA, and that those individuals that still develop the disease experience a delayed onset and reduced severity.[27] Importantly, treatment with the A^q/glycopeptide complex was also successful in relieving symptoms in mice with an established chronic relapsing disease. Although neonatal vaccination with the CII259−273 glycopeptide alone can confer protection against CIA,[28] the therapeutic effect is not as pronounced compared with the glycopeptide/A^q complex and much higher doses of the glycopeptide are required. This is most likely effects of proteolytic degradation and rapid clearance of the glycopeptide in vivo, thereby limiting its use as a therapeutic agent. Development of peptidomimetics with improved proteolytic resistance that are able to mimic the biological activity of the native glycopeptide could circumvent some of these problems. Such peptidomimetics with specific alterations could also be used to study the interactions within the A^q/glycopeptide/TCR

* To whom correspondence should be addressed. Phone: +46-90-7866890 (A.L. and J.K.). Fax: +46-90-138885 (A.L. and J.K.). E-mail: anna.linusson@chem.umu.se (A.L.); jan.kihlberg@chem.umu.se (J.K.).

† Umeå University.

‡ Lund University.

§ AstraZeneca R&D Mölndal.

[a] Abbreviations: RA, rheumatoid arthritis; MHC, major histocompatibility complex; APC, antigen-presenting cell; CII, type II collagen; CIA, collagen-induced arthritis; TCR, T-cell receptor; GalHyl, β-D-galactopyranosyl hydroxylysine; QSAR, quantitative structure-activity relationship; MS, multiple sclerosis; PDB, protein data bank; RMSD, root-mean-square deviation; CLIP, class II-associated invariant chain peptide; IL-2, interleukin-2; RMSG, root-mean-square gradient.

10.1021/jm0705410 CCC: $37.00
Published on Web 10/18/2007

complexes to obtain knowledge of the autoimmune T-cell response in CIA on a molecular level.

Peptidomimetics that inhibit antigen presentation by the human DR1 and DR4 proteins have recently been shown to have a therapeutic effect in transgenic mouse models for both RA and multiple sclerosis (MS).[29] Moreover, peptide epitopes with subtle modifications of TCR contact points, such as substitution of one amino acid, can induce altered T-cell activation states, including anergy where the T cells no longer are responsive to the antigen.[30] Such modified peptides have been used to modulate the T-cell responses and prevent experimental autoimmune encephalomyelitis in a mouse model for MS.[31] Design strategies for modified peptides and peptidomimetics that interact with human or murine class II MHC proteins include introduction of D-amino acids,[32] aza-amino acids,[33] and other non-natural amino acids.[34] Amide bonds in the peptide backbone have also been replaced with various isosteres, such as retro-inverso,[35] methyleneamine,[36] (*E*)-alkene,[37] and ketomethylene[38] isosteres. Furthermore, peptide mimetics based on polypyrrolinone scaffolds,[39] mimicking the polyproline type II conformation of the native peptide ligands, as well as nonpeptidic small organic compounds[40] have been reported to bind to class II MHC proteins. The $Ile^{260}-Ala^{261}$ amide bond of CII260−267 has previously been replaced by a methylene ether isostere, which was found to decrease the binding affinity to the A^q molecule while still allowing some T-cell hybridomas to recognize the A^q/glycopeptide complex weakly.[41,42]

In recent years, several computational tools have emerged that can promote the discovery of new peptide-based vaccines. These include online databases that use predictive algorithms to perform B cell and T cell epitope mapping as well as prediction of MHC binding.[43−45] The design of peptide epitopes with optimized immunogenicity can also be guided by information from a crystal structure of the target class II MHC molecule. Rational design can thus be combined with synthetic chemical methods to develop modified peptides with altered MHC binding and TCR signaling. Although the structure of A^q has not yet been solved by X-ray crystallography, a comparative model of A^q based on the human class II MHC DR1 molecule, which has 63% sequence identity with A^q, has previously been described.[17] In recent years, however, X-ray crystallography has provided several crystal structures of murine class II MHC molecules that are more closely related to A^q.

Here we report a new comparative model of the A^q molecule in complex with CII260−267 that was developed to enable studies of specific molecular interactions. The crystal structure that was used as template had significantly higher sequence identity with A^q and higher resolution, as compared to the previous DR1 template. In a subsequent structure-based design, the amide bond between Ala^{261} and Gly^{262} in the glycopeptide ligand was selected for replacement with $\psi[COCH_2]$, $\psi[CH_2\text{-}NH_2^+]$, and $\psi[(E)\text{-}CH{=}CH]$ isosteres. The three Ala-Gly isostere building blocks were synthesized and subsequently introduced in CII260−267 and the longer glycopeptide CII259−273 using Fmoc-based solid-phase peptide synthesis. The backbone-modified glycopeptides were evaluated for binding to the A^q molecule and recognition by T-cell hybridomas obtained from mice with CIA.

Results and Discussion

Comparative Modeling of the A^q Molecule. Three crystal structures in the Protein Data Bank (PDB)[46] database were found to have more than 90% sequence identity with A^q, that is, two structures of the class II MHC molecule A^b and one of A^d. These structures, determined with resolutions between 2.15 and 2.50 Å, were found suitable as modeling templates because A^b, A^d, as well as A^q have an insertion of two amino acids, that is, β65Pro and β66Glu, that are missing in the other I-A molecules.[47] Backbone alignment of the crystal structures revealed high conformational similarity with root-mean-square deviation (RMSD) values for the α-carbons in the binding sites between 0.59 and 0.75 Å. Importantly, the RMSD values of the two different proteins, A^b and A^d, were in the same range as for the two crystal structures of the same protein (A^b), reflecting a high preservation of the overall 3D structure of these proteins. Additionally, the side chains displayed high conformational similarity, where conserved amino acids were almost identically positioned in the three crystal structures. Amino acids that differed between A^b and A^d, but with side chains having related molecular properties, also adopted strikingly similar conformations. Based on the high sequence identity and conformational similarity of the three suitable templates, the crystal structure with the highest resolution, that is, A^b in complex with a human CLIP peptide (2.15 Å, PDB code: 1MUJ),[47] was selected for the comparative modeling.

In the initial comparative modeling, the side chain conformations of four amino acids in the binding site of A^q, that is, α73Trp, α79Phe, β28Asn, and β37Trp, could not be unambiguously determined, and two rotamers for each side chain were therefore investigated, resulting in 16 models in total. Furthermore, two amino acids (β86Val and α52Thr) in the protein, which also differed from the template, restricted the volume of the P1 pocket as noted after initial attempts of docking the CII260−267 glycopeptide and were therefore adjusted to make the pocket as large as possible. Energy minimization was successfully performed for 13 of the 16 models, and a final comparative model of the A^q molecule was selected based on the ability of the four investigated side chains (i.e., α73Trp, α79Phe, β28Asn, and β37Trp) to participate in favorable interactions. Evaluation of this model revealed that all torsion angles were in allowed regions in the Ramachandran plot and no outliers were detected among the dihedral angles, bond angles, or bond lengths.

Modeling of the CII260−267 Glycopeptide. The modeling studies were focused on the minimal epitope CII260−267, rather than the longer CII259−273 glycopeptide, to facilitate the computational operations by minimizing the number of rotatable bonds in the ligand. The epitope CII260−267 was modeled into the peptide-binding groove using two different strategies; docking and comparative modeling. In the former, 106 different low-energy conformations of the glycopeptide were rigidly docked into the binding site of the A^q comparative model. The binding pose ranked second by the scoring function was consistent with previously experimentally determined binding data.[16,17] The latter approach, where the coordinates of the backbone in the human CLIP peptide found in the A^b crystal structure was used as template to model the backbone of the glycopeptide, also resulted in conformations of the amino acid side chains that fulfilled the evaluation criteria (see Experimental Section). After energy minimization with the A^q molecule, the two binding poses were found to be almost identical in the backbone from Ile^{260} to $GalHyl^{264}$ of the glycopeptide (Figure 1). However, differences were observed in the conformation of the Gln^{267} residue at the C-terminal, which may indicate that this part of the glycopeptide is more flexible in the binding site. The conformation generated by the rigid docking was rotated at the C-terminal, while the pose generated using the backbone

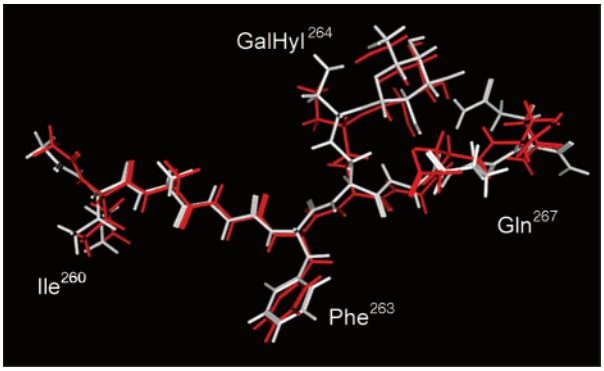

Figure 1. Superposition of two extracted binding poses of the CII260−267 glycopeptide generated by docking (colored red) and comparative modeling (colored gray); here shown after energy minimization with the A^q comparative model.

coordinates of the CLIP peptide displayed an extended conformation throughout the peptide backbone with the Gln^{267} side chain pointing out of the peptide-binding groove. As for other class II MHC proteins, the A^q molecule is capable of binding longer peptides, which is consistent with an extended conformation of the peptide backbone. Consequently, the following studies in this paper are focused on the model having CII260−267 in its extended conformation.

Characterization of the A^q/CII260−267 Complex. As expected, the overall backbone conformation of the modeled A^q molecule in the energy-minimized A^q/CII260−267 complex displayed high structural similarity with the template crystal structure. Backbone alignment of the α-carbons gave RMSD values of 1.06 Å and 0.88 Å for the whole protein and in the binding site, respectively. Also, the conserved amino acids in the binding site of A^q showed high conformational similarity with the crystal structure homolog. The CII260−267 glycopeptide, which bound to A^q with an extended backbone conformation, was positioned deep in the peptide-binding groove, leaving the side chain of GalHyl^{264} only partly extending out of the groove to interact with a TCR (Figure 2). The position of the flexible GalHyl^{264} side chain is somewhat uncertain and structural interpretation of T-cell responses is further complicated by the absence of a TCR in the model. Previous studies have, however, shown that most T-cell hybridomas have a strong dependence on the hydroxyl group at C-4 on the GalHyl^{264} moiety.[15] In the A^q/glycopeptide model this hydroxyl group, that is, HO-4, is the most exposed of all the galactose hydroxyl groups for contacts with a TCR, providing overall support for the extended orientation of GalHyl^{264}. However, it should be noted that a conformation where the GalHyl^{264} side chain instead is flipped in the opposite direction could also lead to an exposed HO-4.

A total of nine areas that bind peptide side chains, referred to as P1−P9, with different properties could be distinguished in the peptide-binding groove, thereby establishing the binding-specificity of A^q. Residues Ile^{260} and Phe^{263} in the CII260−267 glycopeptide were found to be extensively anchored in the prominent P1 and P4 pockets, respectively, as proposed earlier[16,17] (Figure 3a). The well-defined, hydrophobic P1 pocket was formed by residues α31Trp, α43Trp, α32Phe, β85Val, α52Thr, and β82Asn of A^q. Similarly, as in the previous A^q comparative model,[17] the β84aGly residue is positioned in the vicinity of the P1 pocket. The restricted size of this residue probably contributes to making the P1 pocket large enough to accommodate the bulky side chain of Ile^{260} in CII260−267. Analogously, β13Gly, β28Asn, β26Ser, β15Cys, β79Cys,

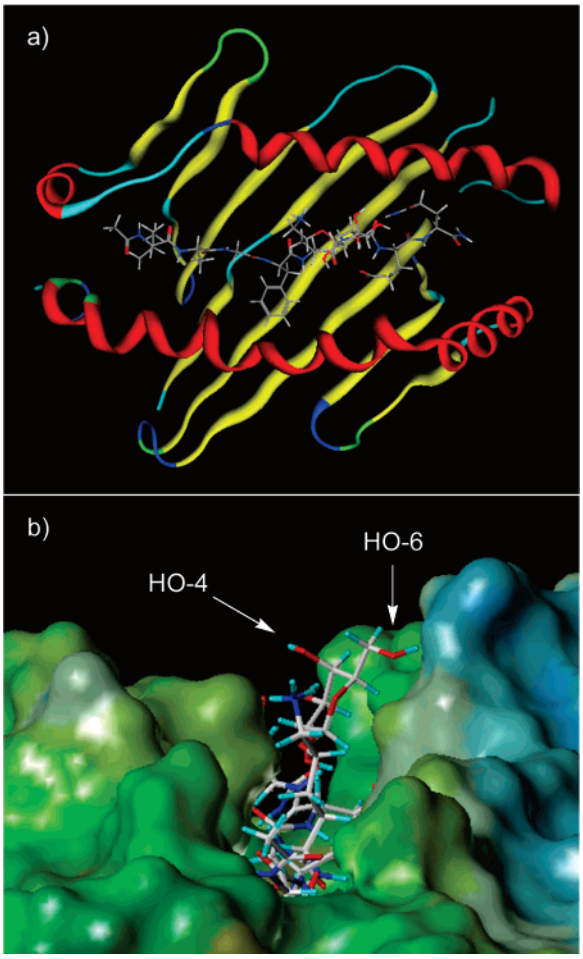

Figure 2. (a) Secondary structure (shown as a ribbon diagram) of the peptide-binding groove of the A^q comparative model with the CII260−267 glycopeptide bound with an extended backbone conformation. (b) The A^q/CII260−267 complex viewed along the peptide-binding groove from the N- to the C-terminal of the glycopeptide and with HO-4 and HO-6 of the GalHyl^{264} moiety indicated. The molecular surface of the A^q molecule is colored blue for polar parts, brown for nonpolar parts, and green for intermediate polarity.

β78Val, and α7Gly established the hydrophobic to medium polarity of the P4 pocket. The amino acids in CII260−267 at positions P3, P6, and P7 were found to be completely or predominantly buried in the A^q binding groove. Gly^{262} was positioned at P3 in a shallow, slightly polar binding area, while the medium-sized, hydrophobic P6 accommodated Gly^{265}. P7 was also found to be quite shallow, where the Glu^{266} side chain in CII260−267 adopted a conformation where it was pointing toward the helical domain rather than toward the β-sheet floor of the binding groove, just as in the A^b/CLIP crystal structure. The glycopeptide side chains Ala^{261}, GalHyl^{264}, and Gln^{267} positioned at P2, P5, and P8, respectively, were solvent exposed. Conformational flexibility of the Gln^{267} residue in the C-terminus of CII260−267 was however indicated in the modeling, as previously stated. The properties of the P2, P3, and P6−P8 binding areas in the modeled A^q structure were consistent with the preferred amino acids in each position suggested by the recently published QSAR model for peptide binding to A^q.[26] The medium-sized P9, which was not occupied by the glycopeptide in the model, was found to be of moderate polarity.

An extensive hydrogen-bonding network was found between the CII260−267 glycopeptide and amino acids in A^q (Figure 3b). A total of 8 out of 13 hydrogen bonds (marked in Figure 3b) that were formed to the glycopeptide backbone were

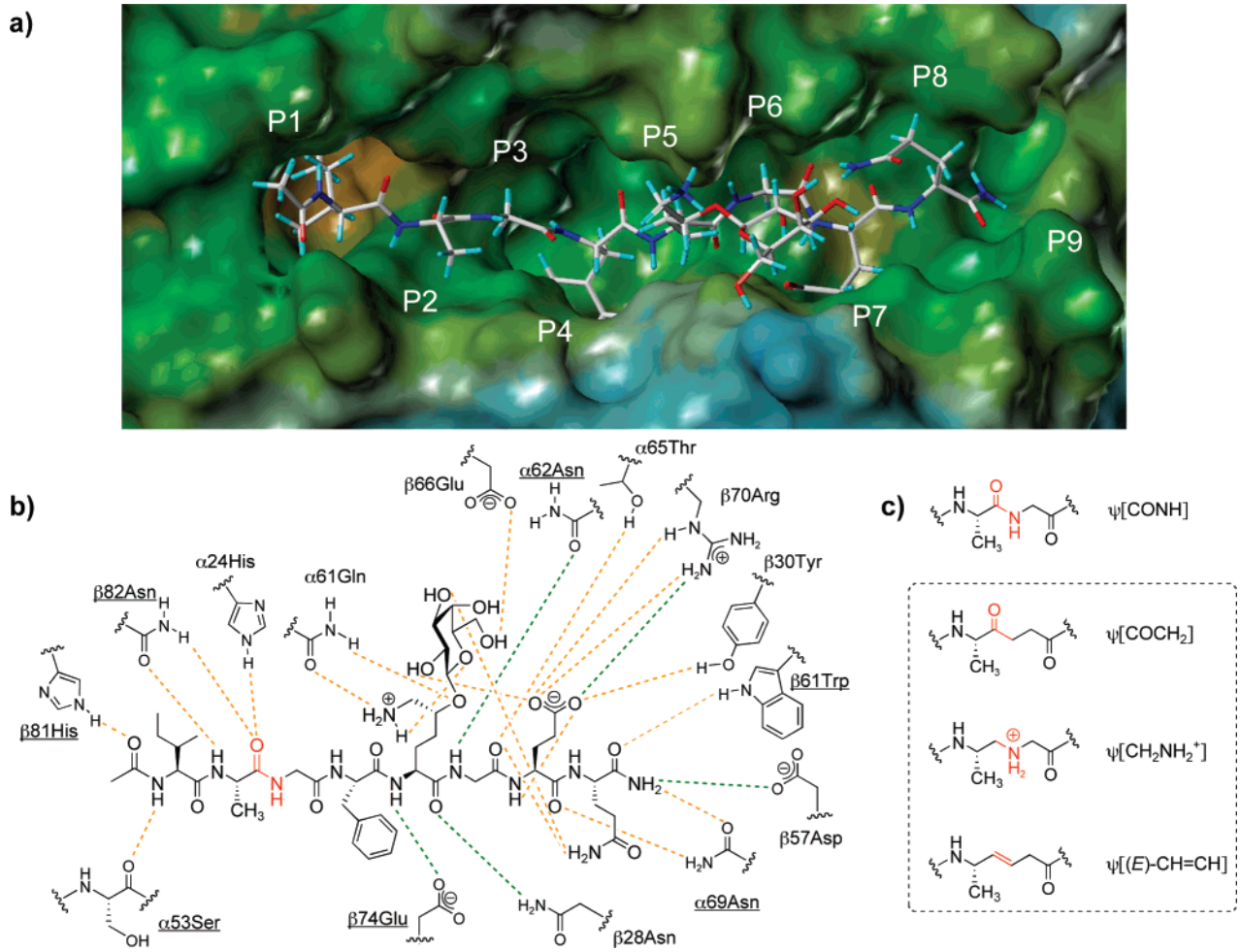

Figure 3. (a) View of the modeled A^q peptide-binding groove with the CII260−267 glycopeptide with an extended backbone conformation. The nine binding areas are denoted P1−P9 (see text for details) and the molecular surface of the A^q molecule is colored blue for polar parts, brown for nonpolar parts, and green for intermediate polarity. (b) The extensive network of hydrogen bonds and ionic interactions found between the CII260−267 glycopeptide and the A^q molecule. The interactions (see Experimental Section for definition) are illustrated with dashed lines and are color coded according to the hydrogen-acceptor distance; orange indicates a distance of 1.4−1.99 Å, while green indicates a distance of 2.0−2.7 Å. Interactions that are conserved in the investigated A^b and A^d crystal structures are indicated by underlined amino acids in the A^q molecule. (c) The three isosteres with varying geometry, charge, and hydrogen-bonding properties that were selected to replace the amide bond between Ala^{261} and Gly^{262} in the glycopeptide backbone.

conserved in the investigated A^b and A^d crystal structures.[47−49] Both amide groups on either side of the important $GalHyl^{264}$ residue were involved in hydrogen bond interactions, thereby contributing to the positioning of this important TCR contact point in the binding site. Previous studies have shown that replacement of Glu^{266} with alanine leaves the T-cell hybridoma HCQ.3 nonresponsive.[42] Somewhat surprisingly, the Glu^{266} side chain was found to be almost completely buried in the binding site in the A^q/CII260−267 model, although it was noted that it formed a hydrogen bond to HO-2 of $GalHyl^{264}$. Interestingly, replacement of HO-2 with a hydrogen atom also led to that the T-cell response was lost for HCQ.3.[15] A possible explanation could thus be that the TCR of HCQ.3 is not in direct contact with the Glu^{266} side chain, but that this residue instead stabilizes the position of the $GalHyl^{264}$ side chain so that an epitope with the proper contact points is presented to the TCR.

Design of Backbone-Modified Glycopeptides. The sequence from Ile^{260} to $GalHyl^{264}$ of CII260−267 contains the most essential features, that is, the anchoring residues and the major TCR contacts required for binding to A^q and for eliciting a T-cell response. Hence, it was attractive to probe the molecular interactions in this part of the ternary A^q/glycopeptide/TCR complexes. Based on the structural information provided by the A^q/CII260−267 model, the Ala^{261}−Gly^{262} amide bond was found to be interesting to modify because its carbonyl group formed two hydrogen bonds to residues in A^q, while the amino group did not participate in any interactions. Isosteric replacement of this amide bond was thus aimed at exploring the interactions within the A^q/glycopeptide/TCR complexes as well as to validate the A^q/glycopeptide model. Isosteres with different hydrogen-bonding properties selected for this study were the ketomethylene ($\psi[COCH_2]$), methyleneamine ($\psi[CH_2NH_2^+]$), and (*E*)-alkene ($\psi[(E)$-CH=CH]) isosteres (Figure 3c). Introduction of the amide bond isosteres in the glycopeptide backbone required synthesis of building blocks **1**−**3** (Figure 4) for subsequent use in Fmoc-based solid-phase glycopeptide synthesis.

Synthesis of Alaψ[COCH$_2$]Gly Isostere 1. The synthetic sequence toward the ketomethylene isostere **1** relied on a strategy previously described by Déziel et al.[50] A key step was the Horner−Wadsworth−Emmons reaction (Scheme 1) between *tert*-butyl glyoxylate[51] and β-ketophosphonate **5**, prepared from methyl ester **4** according to a literature procedure.[50] To minimize racemization, the reaction was initially performed with 1 equiv of *N*-methylmorpholine in dichloromethane at 0 °C.[50] Unfortunately, this rendered alkene **6** in unacceptably low yields

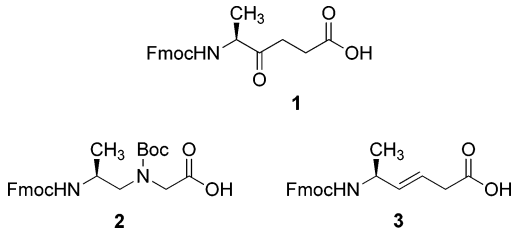

Figure 4. Ala-Gly isostere building blocks protected for solid-phase synthesis of backbone-modified type II collagen glycopeptides.

Scheme 1. Synthesis of the Alaψ[$COCH_2$]Gly Isostere[a]

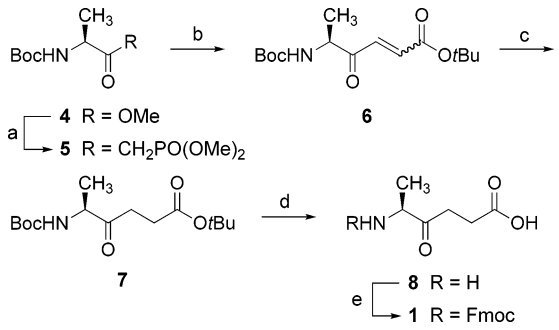

[a] Reagents and conditions: (a) cf. ref 50; (b) *tert*-butyl glyoxylate,[51] TEA, LiCl, MeCN, 0 °C, 97% as an isomeric mixture of *E*/*Z* 3:1; (c) H_2, Pd/C, EtOAc, rt, 81%; (d) TFA, CH_2Cl_2, rt; (e) FmocOSu, $NaHCO_3$, acetone, H_2O, rt, 88% from **7**.

Scheme 2. Synthesis of Mosher Amides[a]

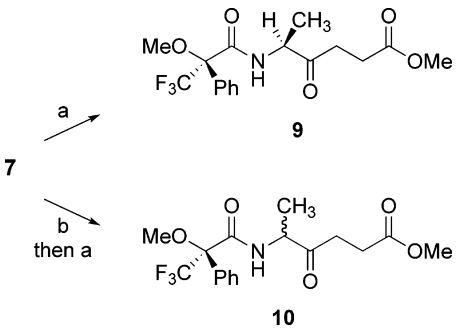

[a] Reagents and conditions: (a) (i) TFA, CH_2Cl_2, rt; (ii) TMSCl, MeOH, rt; (iii) (*S*)-MTPA-Cl, DIPEA, CH_2Cl_2, rt; (b) DBU, THF, 80 °C.

(<22%), although exclusively as the *E*-isomer. By instead using 1 equiv of triethylamine and lithium chloride[52] in acetonitrile at 0 °C an excellent yield of **6** (97%) was obtained as a diastereomeric mixture (*E*/*Z* 3:1) according to ^{1}H NMR analysis.[51] Separation of the two diastereomers was not required because the alkene functionality was subsequently reduced by hydrogenation over palladium on charcoal to afford the corresponding saturated isostere **7** in 81% yield.[53] Simultaneous cleavage of the Boc-group and the *tert*-butyl ester followed by Fmoc-protection then afforded the desired building block **1** (88% from **7**).

It had previously been reported that the Horner−Wadsworth−Emmons reaction between benzyl glyoxylate and **5** under similar conditions (i.e., 2 equiv of triethylamine in acetonitrile at room temperature) was accompanied by racemization of the stereocenter.[50] To investigate how the modified reaction conditions used in the synthesis of **6** had influenced the degree of racemization, Mosher amide[54] **9** was synthesized from **7** (Scheme 2). A reference 1:1 diastereomeric mixture of Mosher amides **10** was prepared analogously from racemic **7**. Integration of the signals from the diastereomeric methyl groups in the ^{1}H NMR spectrum of **9** established that the diastereoselectivity was

Scheme 3. Synthesis of the Alaψ[$CH_2NH_2^+$]Gly Isostere[a]

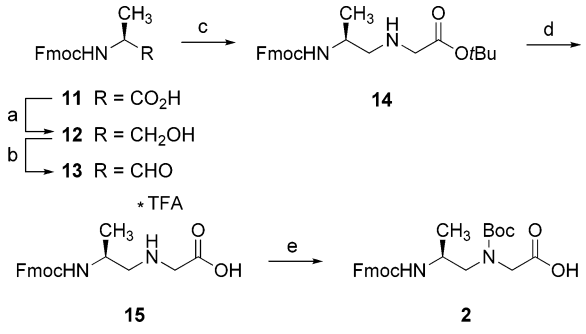

[a] Reagents and conditions: (a) cf. refs 55 and 56; (b) Dess-Martin periodinane, CH_2Cl_2/DMSO 1:1, rt; (c) HCl·H-Gly-O*t*Bu, $NaBH(OAc)_3$, CH_2Cl_2, MeOH, rt, 43% from **12**; (d) TFA, CH_2Cl_2, rt; (e) Boc_2O, DIPEA, CH_2Cl_2, rt, 89% from **14**.

>100:1 and it was thus concluded that no significant degree of epimerization had occurred (see Supporting Information).

Synthesis of Alaψ[CH_2N(Boc)]Gly Isostere 2. The synthetic route toward the orthogonally protected methyleneamine isostere **2** involved reductive amination as a key step (Scheme 3). Alcohol **12**[55] was first prepared from *N*-Fmoc-protected L-alanine (**11**) via reduction of the corresponding mixed *iso*-butyl anhydride using sodium borohydride according to a published one-pot procedure.[56] After workup, **12** was directly oxidized to aldehyde **13** by treatment with Dess−Martin periodinane.[57] This oxidation was performed in dichloromethane/dimethyl sulfoxide (1:1) due to solubility problems. To minimize racemization of the stereocenter, **13** was kept cold during workup and was used directly without further purification.[58,59] Thus, reductive alkylation[60] of glycine *tert*-butyl ester with **13** using sodium triacetoxyborohydride as reducing agent afforded secondary amine **14** in a modest yield (43% from **12**). Deprotection of the carboxylic acid to give **15** required stirring overnight in trifluoroacetic acid/dichloromethane (1:3), and this was followed by Boc-protection of the secondary amine to afford carboxylic acid **2** (89% from **14**).

Synthesis of Alaψ[(*E*)-CH═CH]Gly Isostere 3. Wiktelius et al. have developed a synthetic route to the Pheψ[(*E*)-CH═CH]Phe isostere relying on a Wittig-type reaction with excellent *E*-selectivity for the Phe−Phe derivative.[61] This methodology was applied to the synthesis of Alaψ[(*E*)-CH═CH]Gly isostere **3**, which allowed investigation of the selectivity in the Wittig reaction for a derivative with less bulky side chains.

Phosphonium salt **19** was prepared in three steps from L-alaninol in 62% overall yield (Scheme 4). Unfortunately, small impurities of triphenylphosphine oxide (~3.5%) could not be removed in the purification of **19**. In the Wittig reaction, **19** was first treated with 2 equiv of *n*-butyllithium to generate the ylide and to lithiate the amide.[61] Subsequent addition of *tert*-butyldiphenylsilyl-protected β-hydroxipropionic aldehyde[62−64] at −78 °C was followed by slowly raising the temperature to 0 °C to allow equilibration of the alkene to the *E*-isomer. This resulted in formation of **20** in 80−89% yield, but disappointingly, the *E*/*Z* ratios varied between 3:2 and 2:3. No effect of the counterion on the selectivity was observed when the bromide corresponding to **19** was employed instead. Because the alkene isomers could not be separated by flash chromatography, the mixture was treated with tetrabutylammonium fluoride to afford the corresponding alcohols. According to TLC, this deprotection appeared to be quantitative, however, repeated purification by flash chromatography to separate **(*E*)-21** and **(*Z*)-21** resulted in only modest yields (29% and 30%, respectively, when starting from a mixture of **20** with *E*/*Z* 1:1). In the following step,

Scheme 4. Synthesis of Alaψ[(*E*)-CH═CH]Gly and Alaψ[(*Z*)-CH═CH]Gly Isosteres[a]

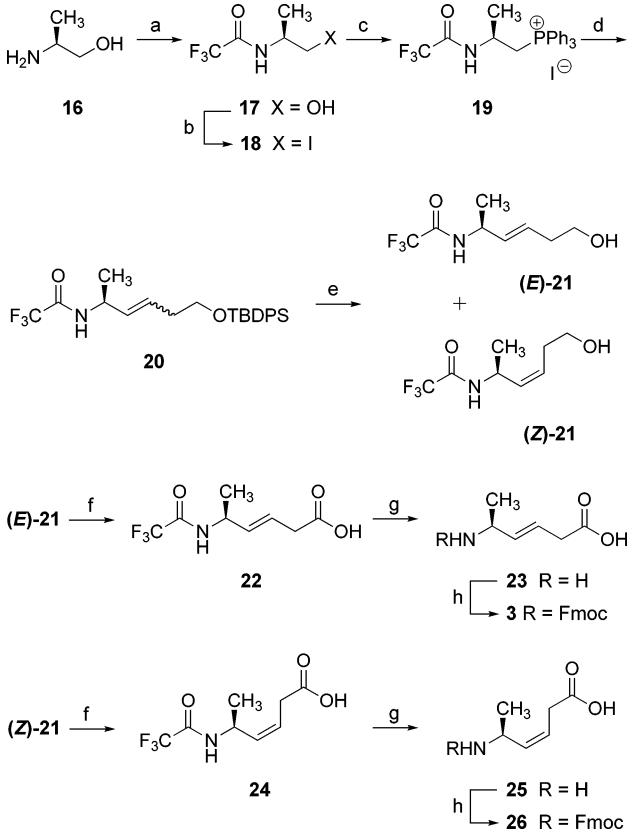

[a] Reagents and conditions: (a) TFAA, TEA, CH_2Cl_2, 0 °C, 78%; (b) I_2, PPh_3, imidazole, toluene, rt, 79%; (c) PPh_3, toluene, reflux, quantitative yield; (d) (i) 2 equiv *n*-BuLi, THF, −78 °C → rt → −78 °C; (ii) $TBDPSO(CH_2)_2CHO$,[62−64] THF, −78 °C → 0 °C, 80−89% as isomeric mixtures of *E*/*Z* 3:2−2:3; (e) TBAF, THF, rt, **(*E*)-21** (29%) and **(*Z*)-21** (30%); (f) CrO_3, 4.4 M H_2SO_4 (aq), acetone, rt, 92% for **22**, 87% for **24**; (g) K_2CO_3, MeOH, H_2O, rt; (h) FmocOSu, MeCN/Na_2CO_3 (10% aq) 1:1, rt, 89% for **3** from **22**, 86% for **26** from **24**.

alcohol **(*E*)-21** was oxidized to carboxylic acid **22** in 92% yield by treatment with Jones' reagent. This reaction was carefully monitored to minimize the formation of unidentified byproducts that could not be removed in the following purification step. Deprotection of the amino group using aqueous potassium carbonate and methanol, followed by immediate Fmoc-protection afforded the desired building block **3** (89% from **22**). Due to lack of *E*-selectivity in the Wittig reaction, this reaction sequence could also provide the Alaψ[(*Z*)-CH═CH]Gly building block **26**, which was subsequently incorporated in the glycopeptide backbone. Thus, building block **26** was synthesized from **(*Z*)-21** in 75% yield over three steps according to the same procedure as described for **3**.

Synthesis of Backbone-Modified Glycopeptides. The immunological studies were initially focused on the minimal epitope CII260−267 (**27**), and building blocks **1** and **2** were therefore introduced in its backbone to give **28** and **29**, respectively (Scheme 5). However, use of the longer glycopeptide CII259−273 could also allow studies of the human class II MHC protein DR4 because its epitope is shifted three amino acids toward the C-terminus as compared to peptides bound by the murine A^q molecule.[65] Thus, all isostere building blocks, that is, **1**−**3** and **26**, were incorporated instead of residues Ala^{261}−Gly^{262} in the CII259−273 glycopeptide **30** to give **31**−**34**. The modified glycopeptides were synthesized on solid phase under standard conditions[19] according to the Fmoc protocol. Glycopeptides **31**−**34** were synthesized with charged termini, while the truncated glycopeptides **28** and **29** were synthesized as C-terminal amides and with acetylated N-terminals to avoid positioning glycopeptides with charged termini in the binding site of A^q. An orthogonally protected galactosylated hydroxylysine derivative, which was prepared according to a published procedure[66] but with some modifications (see Supporting Information), was used in the syntheses.

An initial attempt to synthesize glycopeptide **28**, containing the ketomethylene isostere, relied on coupling of Fmoc-protected isoleucine at the N-terminal followed by Fmoc deprotection and acetylation. However, this rendered a complex mixture of products after cleavage from the solid phase, with the major product being the ring-closed analogue **35**, as indicated by mass spectrometry and NMR spectroscopy (Figure 5). Formation of **35** could be explained by nucleophilic attack of the α-amino group in isoleucine on the ketone of the isostere, resulting in formation of an imine[38] followed by oxidation. This side reaction was efficiently avoided by coupling of Ac-Ile-OH at the N-terminus in the synthesis of **28**, whereas Boc-Gly-Ile-OH was coupled in the synthesis of **31**. Gratifyingly, this strategy would also minimize epimerization of the stereocenter in the isostere during solid-phase synthesis by avoiding treatments with piperidine that previously has been reported to epimerize Cα of other ketomethylene isosteres.[67]

The glycopeptides were cleaved from the solid support followed by deacetylation of the galactose moiety by treatment with methanolic sodium methoxide; a reaction that was carefully monitored by analytical reversed-phase HPLC. Unfortunately, the deprotection conditions led to epimerization of the base-sensitive stereocenter in the ketomethylene isostere in glycopeptides **28** and **31**. However, it was found that the rate of deacetylation was much faster than the epimerization.[68] Hence, by performing the deacetylation in several small portions under

Scheme 5. Structures of the Backbone-Modified Glycopeptides Derived from Type II Collagen

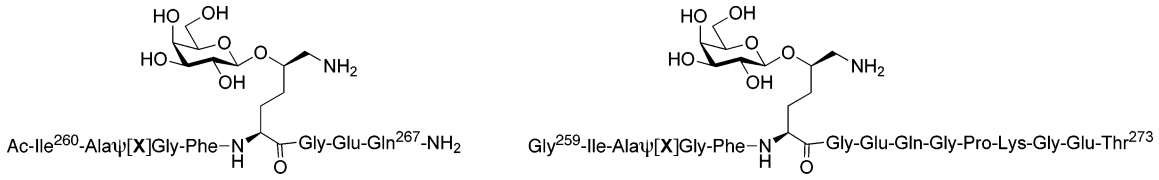

	27	**X** = CONH	
1	**28**	**X** = $COCH_2$	
2	**29**	**X** = $CH_2NH_2^+$	
	30	**X** = CONH	
1	**31**	**X** = $COCH_2$	
2	**32**	**X** = $CH_2NH_2^+$	
3	**33**	**X** = (*E*)-CH=CH	
26	**34**	**X** = (*Z*)-CH=CH	

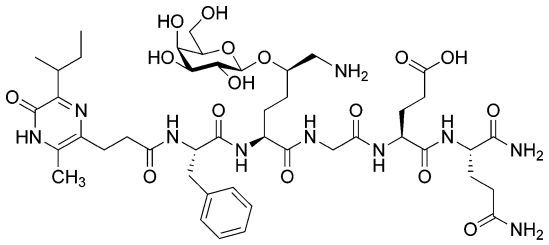

35

Figure 5. Structure of the major product formed in the initial attempt to synthesize glycopeptide **28**, which contains the ketomethylene isostere.

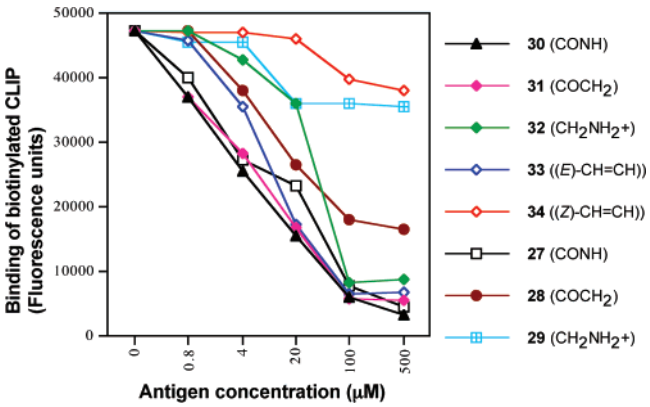

Figure 6. Binding of a fixed concentration of biotinylated CLIP peptide to recombinant A^q proteins in a competitive binding assay with increasing concentrations of the backbone-modified glycopeptides **28**, **29**, and **31**−**34**, or the native glycopeptides **27** and **30**. A^q-bound biotinylated CLIP was detected in a time-resolved fluoroimmunoassay using europium-labeled streptavidin. The values represent the average from duplicates.

a limited reaction time, epimerization was minimized and the minor diastereomer could successfully be removed during the subsequent purification by reversed-phase HPLC. Analytical reversed-phase HPLC also revealed that crude glycopeptides **29** and **32** each consisted of two main products in a ratio of 4:1, and after separation, both compounds were established to have the correct mass. This isomeric mixture was most likely due to racemization of the sensitive stereocenter in aldehyde **13** during synthesis of the methyleneamine building block **2**. Importantly, all traces of the minor diastereomers were successfully removed in the purification to give both **29** and **32** as pure isomers.

After purification by reversed-phase HPLC, the backbone-modified glycopeptides **28**, **29**, and **31**−**34** were obtained in 7−26% overall yields based on the resin capacities and in 98−100% purity. All glycopeptides were homogeneous according to analytical reversed-phase HPLC using two eluent systems, and their structures were confirmed by ^{1}H NMR spectroscopy and MALDI-TOF mass spectrometry.

Binding to the Class II MHC A^q Molecule. The ability of the backbone-modified (**28**, **29**, and **31**−**34**) and native (**27** and **30**) glycopeptides to bind to the class II MHC A^q molecule was studied in a competitive binding assay. Increasing concentrations of each glycopeptide were incubated with a fixed concentration of biotinylated CLIP peptide and recombinant A^q protein, and the amount of A^q-bound biotinylated CLIP was then quantified in a time-resolved fluoroimmunoassay (Figure 6). It was found that the CII259−273 glycopeptides incorporating the ketomethylene (**31**), methyleneamine (**32**), and (*E*)-alkene (**33**) isosteres completely inhibited binding of the biotinylated CLIP peptide at the 100 μM concentration, just as native **30**. However, at 4 μM concentration only ketomethylene **31** bound to A^q as efficiently as the nonmodified glycopeptide **30**. At this concentration, a reduction in the binding efficiency was observed for (*E*)-alkene **33**, whereas methyleneamine **32** displayed almost no A^q binding. As expected, the (*Z*)-alkene modification in **34** resulted in a complete loss of binding to A^q even at the highest tested concentrations.

In the A^q/CII260−267 model, two hydrogen bonds were formed between the carbonyl group in the Ala^{261}−Gly^{262} amide bond and the β82Asn and α24His residues in A^q (Figure 3b). The hydrogen bond involving the β82Asn is conserved in other class II MHC A/peptide complexes.[47−49] The ketomethylene isostere in **31** is able to retain these hydrogen-bonding interactions, and its increased flexibility compared to the amide bond did not seem to affect the A^q binding ability. The hydrophobic and rigid (*E*)-alkene in **33**, on the other hand, is successful in mimicking the geometry of the amide bond but is not able to participate in any hydrogen-bonding interactions and is not favored by the polar character of the binding site at this position. (*E*)-Alkene **33** still displayed good binding to A^q, despite the loss of two hydrogen bonds, suggesting that this glycopeptide is bound in a conformation that successfully retains other important interactions. However, the loss of binding that was observed at low concentrations of **33** indicates that the carbonyl group in the Ala^{261}−Gly^{262} amide bond is engaged in interactions that, although not critical for A^q binding, do contribute to the affinity of the glycopeptide/A^q complex. The importance of hydrogen bonding to the peptide backbone has previously been studied for a diverse set of peptides that bind to the A^d molecule.[69] It was found that selective mutations of residues in A^d that hydrogen bonded to the peptide ligand increased the dissociation rates of the complexes by 4- to 1000-fold. The hydrogen-bonding interactions at the peptide N-terminal were particularly important for the binding stability.

The significant reduction in binding observed for methyleneamine **32** at 20 μM and lower concentrations is most likely caused to a large extent by localization of a charged group in an unfavorable position in the peptide-binding groove of A^q. In addition, **32** is more flexible than the amide bond and is unable to form the hydrogen bonds that the carbonyl group of the Ala^{261}−Gly^{262} amide bond is involved in. As expected, (*Z*)-alkene **34** displayed only a very weak ability to bind to A^q at high concentrations, which is most likely explained by the stereochemistry of the alkene that distorts the extended backbone conformation in between the two anchoring residues. The simultaneous positioning of the Ile^{260} and Phe^{263} side chains in the P1 and P4 pockets of A^q is thereby prevented.

The truncated CII260−267 backbone-modified glycopeptides **28** and **29** displayed the same trends in binding to A^q as their extended counterparts. The effects were, however, more pronounced in these shorter sequences, probably because fewer interaction points in total are present that may compensate for any loss of interactions, as a consequence of the introduced isosteres. Compared to the corresponding reference **27**, a reduction in binding was observed for ketomethylene **28** at all tested concentrations. The methyleneamine isostere in **29** was found to only have a very weak ability to bind to A^q.

Recognition by T-Cell Hybridomas. The ability of the isosteric glycopeptides **28**, **29**, and **31**−**34**, as well as the native **27** and **30**, to induce an immune response was studied using a panel of carbohydrate-dependent and A^q-restricted T-cell hybridomas obtained from mice with CIA. The hybridomas were selected from five groups previously established to have different

Table 1. Immune Response of T-Cell Hybridomas When Incubated with Antigen-Presenting Spleen Cells Expressing A^q and Increasing Concentrations of Glycopeptides **27**−**34**[a,b]

sequence		CII259−273					CII260−267		
hybridoma	group[c]	**30** (CONH)	**31** ($COCH_2$)	**32** ($CH_2NH_2^+$)	**33** ((*E*)-CH═CH))	**34** ((*Z*)-CH═CH))	**27**[d] (CONH)	**28** ($COCH_2$)	**29** ($CH_2NH_2^+$)
HD13.9	1	+++	+++	−	−	−	++	++	−
HD13.10	1	++++	+++	−	−	−	+++++	+++	−
HNC.1	1	++++	++	−	−	−	+++	+	−
HCQ.10	2	+++	−	−	−	−	++++	−	−
HCQ.2	3	++++	+++	−	+	−	+++++	++	−
HCQ.3	3	+++++	+++	−	+	−	++++++	++	−
HCQ.6	3	+++++	+++	−	+	−	++++++	++	−
HM1R.2	4	+++	++	−	−	−	+++	+	−
22a1-7E	5	+++(+)	++	−	−	−	+++	+	−

[a] The T-cell response data and the corresponding dose−response curves are provided in the Supporting Information. [b] The magnitude of the responses were determined from the concentration of antigen required to induce secretion of IL-2 corresponding to 6% of the max response for the native CII259−273 glycopeptide **30**: − = no response; + = 20 μM; ++ = 4 μM; +++ = 0.8 μM; ++++ = 0.16 μM; +++++ = 0.032 μM; ++++++ = 0.0064 μM; (+) = just below the threshold. [c] Groups of hybridomas with different specificity for the hydroxyl groups on the $GalHyl^{264}$ moiety.[15] [d] The native CII260−267 glycopeptide **27** was tested on a separate plate and the magnitude of its response was determined compared to the response induced by reference **30** on the same plate according to the criteria stated above.

specificity for the hydroxyl groups on the $GalHyl^{264}$ moiety.[15] The glycopeptides were incubated with antigen-presenting spleen cells expressing A^q and each of the selected hybridomas. Recognition of the A^q/glycopeptide complex on the cell surface by a T-cell hybridoma results in secretion of interleukin-2 (IL-2) into the medium, which was quantified in an ELISA.

As expected, all T-cell hybridomas elicited strong responses when stimulated with the native glycopeptide **30** in complex with the A^q molecule (Table 1). Presentation of the ketomethylene-modified glycopeptide **31** by A^q molecules led to IL-2 secretion by eight out of nine T-cell hybridomas, representing four out of five groups but, compared to the native A^q/**30** complex, the responses were weaker. Interestingly, the A^q/**31** complex failed to stimulate HCQ.10, indicating that the interactions between its TCR and A^q/**31** have been altered as compared to A^q/**30**. The inability of **31** to activate HCQ.10 could indicate that its TCR depends on interactions with the proton in the Ala^{261}−Gly^{262} amide bond of **30**. Although this proton is pointing up toward the TCR in the modeled A^q/CII260−267 complex, it is still positioned deep down in the peptide-binding groove, making it somewhat uncertain if direct contact is possible. The reduced stimulation may also be explained by a subtle change of the conformation of the A^q-bound glycopeptide induced by the isostere that, as a consequence, results in presentation of a slightly different epitope, affecting other interaction points with the TCR of HCQ.10. The T-cell responses of the different hybridomas displayed the same trends for the truncated ketomethylene-modified glycopeptide **28** when bound to A^q as for **31**, but the responses were even weaker, most likely due to the lower affinity of **28** for the A^q molecule.

Although the (*E*)-alkene in **33** was well-tolerated in binding to A^q, it was found to have a drastic effect on the interactions with the different T-cell hybridomas. Only the three hybridomas belonging to group 3 secreted low amounts of IL-2 upon stimulation at the highest concentration of **33**. The remaining five hybridomas, which recognized both **31** and **28** when bound to A^q, displayed a complete loss of T-cell response when instead presented to the A^q/**33** complex. Isostere **33** is unable to retain the two hydrogen bonds that, according to the A^q/CII260−267 model, were formed between residues in A^q and the carbonyl group in the Ala^{261}−Gly^{262} amide bond. As a consequence, we propose that the conformation of **33** is adjusted in the A^q peptide-binding groove to compensate for positioning of the alkene in the polar environment that is normally occupied by the Ala^{261}−Gly^{262} amide bond, thus resulting in the presentation of an altered T-cell epitope. A contributing factor to the lack of signal transduction could also be the inability of the TCRs to directly interact with an amide proton at the modified position in **33**.

A previous study has shown that E^k binding glycopeptides with amino acid substitution and small differences in the TCR exposed carbohydrate moiety induced drastically altered TCR signaling.[70] It was found that the levels of secreted IL-2 that was triggered by the analogues could be linked to different phosphorylation patterns in the signal transduction machinery of the TCR. Other studies have correlated the ability of a class II MHC/peptide complex to activate a TCR with the dissociation rate of the MCH/peptide/TCR complex.[71−73] A somewhat slower dissociation rate was required for complete phosphorylation and thereby efficient T-cell stimulation, while dissociation rates at the faster end of the scale resulted in partial activation or even deactivation. Studies to elucidate the phosphorylation patterns and the rates of dissociation have not been performed for the backbone-modified glycopeptides described in this article. However, based on the findings from such studies, it is possible that an adjustment of the A^q-bound conformation of (*E*)-alkene **33** could confer presentation of a slightly altered T-cell epitope that in turn affect the interactions with the TCRs leading to faster dissociation rates for the MHC/glycopeptide/TCR complexes. Thus, incomplete or lack of phosphorylation then results in partial or no activation of the TCRs, respectively, as was seen for A^q/**33** and the T-cell hybridomas included in the present study. Methyleneamine **32**, which displayed a significant reduction in A^q binding, failed to stimulate any of the T-cell hybridomas. As expected, the T-cell hybridomas did not show any stimulation either on incubation with the corresponding truncated methyleneamine analogue **29** or the (*Z*)-alkene containing **34**, which displayed very weak and almost no binding to A^q, respectively.

In summary, our data show that very small structural changes in the glycopeptide backbone can have striking effects on the interactions with different TCRs and thereby on T-cell activation. Such sensitivity of TCRs when interacting with various backbone-modified and amino acid-substituted peptides bound to other murine class II MHC proteins have been encountered in several recent studies.[35−38,70,73] The different responses displayed by the T-cell hybridomas investigated in this study have not yet been correlated to their effect in vivo. Thus, it would be highly interesting to evaluate the ability of ketomethylene **31** and (*E*)-alkene **34**, that both bind well to A^q, to induce tolerance in mice with CIA in vaccination studies. These

could be performed either with the glycopeptide alone or in complex with soluble A^q proteins.

Conclusions

In this study, a new comparative model of the murine class II MHC A^q molecule in complex with the CII260−267 glycopeptide has provided a detailed structural basis for understanding antigen presentation by A^q. The CII260−267 glycopeptide, positioned deep in the binding groove of A^q, was firmly anchored by the Ile^{260} and Phe^{263} residues in the P1 and P4 pockets, respectively. This left the $GalHyl^{264}$ side chain, which is a critical TCR contact point, partially extending out of the groove. On the basis of the A^q/CII260−267 model, the Ala^{261}−Gly^{262} amide bond in the glycopeptide backbone was selected for replacement by $\psi[COCH_2]$, $\psi[CH_2NH_2^+]$, and ψ-[(*E*)-CH═CH] isosteres. Fmoc-protected Ala-Gly isostere building blocks were successfully synthesized and introduced in two sets of glycopeptides from rat CII based on the CII259−273 and the CII260−267 sequences.

The ability of the modified glycopeptides to bind to A^q and to stimulate T-cell hybridomas was evaluated and then interpreted in view of the structural features of the A^q/glycopeptide model. It was found that the ketomethylene isostere, being the only isostere able to retain the two hydrogen bonds formed to the Ala^{261}−Gly^{262} amide bond, bound to A^q as efficiently as the native glycopeptide. The (*E*)-alkene isostere also bound well, while the other modifications had various degrees of detrimental effects on binding. Evaluation of the ability of the modified glycopeptides to stimulate a panel of T-cell hybridomas revealed that the TCRs were very sensitive for the isosteric modifications. While the ketomethylene isostere was able to stimulate eight out of nine T-cell hybridomas (four out of five groups) to various extents, the (*E*)-alkene gave only weak responses for three hybridomas belonging to the same group. It was reasoned that the introduction of an (*E*)-alkene isostere probably conferred changes in the conformation of the glycopeptide when bound by A^q, thereby causing a different epitope to be presented to the TCRs. It is also possible, but less likely, that a direct loss of hydrogen-bonding interactions with the TCRs at the position of the original Ala^{261}−Gly^{262} amide bond contributes to the altered T-cell response.

In conclusion, novel backbone-modified glycopeptides have been used to probe the interactions in ternary A^q/glycopeptide/TCR complexes to investigate the molecular mechanisms governing activation of autoreactive T cells in CIA. The results obtained in this study can be further used in the design of new glycopeptide mimetics with increased stability toward proteolytic degradation in vivo, potentially rendering structures that can give protective effects when used in vaccination studies in CIA.

Experimental Section

Comparative Modeling. The modeling was performed using the Molecular Operating Environment[74] (MOE) software and the AMBER94 force field with an implicit distance dependent dielectric solvation model. Default parameter settings were used in the computational operations, unless otherwise stated. The amino acid sequence of the A^q protein was retrieved from the Swiss-Prot/TrEMBL[75] database (accession numbers, α-chain: P04227, β-chain: P06342). Amino acids DHVGFY were added at the N-terminal of the α-chain. The BLAST[76] program was used to search the PDB[46] database for crystal structures with more than 90% sequence-identity with both the α- and β-chain of the A^q protein. The resulting complexes (PDB codes: 1MUJ,[47] 2IAD,[48] and 1LNU)[49] were superposed by backbone alignment using the MOE[74] software and their similarity was compared both visually and by calculation of RMSD values before selecting a template. The coordinates for seven amino acids (residues from β105Arg to β111His) in the β-chain of the template crystal structure (PDB code: 1MUJ[47]) were missing. These amino acids were located far away from the binding site and were therefore considered to be of no relevance for the modeling. The sequences of the α- and β-chain of A^q were separately aligned with their corresponding template sequence using the blosum62 substitution matrix.[74] Ten independent models were constructed for each chain based on a Boltzmann-weighted randomized modeling procedure as implemented in MOE with no energy minimization. The coordinates for the backbone and the side chains of conserved amino acids were directly copied from the template crystal structure. For the amino acids in A^q that differed from the template, 10 side chain conformations were suggested using a rotamer library in MOE. All models of the α- and β-chains were superposed and side chain conformations were selected for those amino acids that differed from the template in the binding site. This selection was guided by the indicated rotamer preference found in all crystal structures with more than 90% sequence identity. In those cases where the side chain conformations could not be unambiguously determined, several rotamers were chosen to represent the suggested conformations. The α- and β-chains were combined to give all possible combinations of the side chain conformations and subjected to further analysis. Reduce[77] was used to add hydrogens to the molecules followed by energy minimization using a combination of three methods; steepest descent, conjugate gradient, and truncated Newton, as implemented in MOE. The minimizations were terminated when the root-mean-square gradient (RMSG) was <0.1, current geometry was used as chiral constraint, and a quadratic force was applied on the backbone atoms with a force constant of 100. The side chain of β86Val was kept fixed during the energy minimization to prevent it from readopting its initial conformation (see Results and Discussion). After visual inspection of the minimized models, a final comparative model of the A^q molecule was chosen based on the ability of the amino acid side chains to participate in hydrogen bonds, hydrophobic and π-interactions, as well as steric factors. The numbering of amino acids in the A^q molecule is consistent with those used for A^b, A^k, HLA-DR, and I-E. Hydrogen bonds were defined to have a distance of ≤3.0 Å between a hydrogen of a donor atom D and an acceptor atom A, and to have a D−H···A angle of 120−180°.

Modeling of the CII260−267 Glycopeptide. Docking: The BABEL[78] file format converter was used to represent the CII260−267 glycopeptide as chiral SMILES,[79] from which the 3D atomic coordinates were generated using the CORINA[80] software. This conformation was used as input in a conformational search using OMEGA[81] with the parameters *ewindow*, *rms*, and *maxconfs* set to 14, 1.0, and 5000, respectively. The generated ensemble of ligand conformations was docked into the binding site of the comparative A^q model using the FRED[82] program. The parameter settings *tstep* 1.25, *rstep* 1.0, *clash_checking* 0.5, *neg_img_size* large, and chemgauss as scoring function were selected based on previous optimization studies.[83] The 20 highest-ranked conformations by the scoring function were subjected to visual inspection and manual ranking based on the following criteria: the side chains of Ile^{260} and Phe^{267} positioned deeply in the P1 and P4 pockets, respectively, an extended backbone conformation, and the galactose moiety pointing out of the binding site as supported by experimentally determined data.[15−17] The highest manually ranked conformation was energy-minimized with the A^q molecule using MOE until the RMSG was <0.01 and applying current geometry as chiral constraint. **Comparative Modeling:** The sequence of CII260−267 (with Lys^{264} instead of $GalHyl^{264}$) was manually aligned with the template CLIP[47] sequence so that the anchoring residues in the respective P1 and P4 pocket matched. A total of 100 independent comparative models were then constructed for CII260−267 using the same parameter settings as previously described for the modeling of the A^q molecule. Selection of side chain conformations in CII260−267 was guided by the indicated rotamer preference of the ligand found in the template and two other crystal structures,[48,49] as well as in the conformation of CII260−267 obtained when

docking with FRED. The ability to participate in hydrogen bonds, hydrophobic and π-interactions, as well as steric factors with the A^q molecule were also considered. Manual hydroxylation and subsequent glycosylation of the Lys[264] side chain, acetylation of the N-terminal and amidation of the C-terminal, were followed by energy minimization with the A^q molecule until the RMSG was <0.01.

General Synthetic Procedures. All reactions were carried out under an inert atmosphere with dry solvents under anhydrous conditions, unless otherwise stated. CH_2Cl_2 and MeCN were distilled from calcium hydride, whereas THF was distilled from potassium. DMF was distilled under reduced pressure and then dried over 3 Å molecular sieves. MeOH was dried over 3 Å molecular sieves. TLC analysis was performed on silica gel 60 F_{254} (Merck) with detection by UV light and staining with phosphomolybdic acid in ethanol, phosphomolybdic acid and $Ce(SO_4)_2$ in aqueous H_2SO_4 or alkaline aqueous $KMnO_4$, followed by heating. After workup, organic phases were dried over Na_2SO_4 before being concentrated under reduced pressure. Flash column chromatography was performed on silica gel (Matrex, 60 Å, 35−70 μm, Grace Amicon). Optical rotations were measured with a Perkin Elmer model 343 polarimeter at 20 °C. ^{1}H and ^{13}C NMR spectra for the Ala-Gly isostere building blocks and their intermediates were recorded at 298 K on a Bruker DRX-400 spectrometer at 400 and 100 MHz, respectively, and calibrated using the residual peak of solvent as internal standard [$CDCl_3$ ($CHCl_3$ δ_H 7.26 ppm, $CDCl_3$ δ_C 77.0 ppm) or CD_3OD (CD_2HOD δ_H 3.31 ppm, CD_3OD δ_C 49.0 ppm)]. First-order chemical shifts and coupling constants were obtained from one-dimensional spectra; carbon and proton resonances were assigned from COSY and HETCOR experiments. Signals that could not be assigned are not reported. Spectra for the glycopeptides were recorded at 298 K on a Bruker Avance spectrometer at 500 MHz in H_2O/D_2O (9:1) with H_2O (δ_H 4.76) as internal standard. COSY, TOCSY, and ROESY experiments were used for assignment of signals and determination of chemical shifts. Analytical reversed-phase HPLC was performed on a Beckman System Gold HPLC equipped with either a Kromasil C8 column (250 × 4.6 mm, 5 μm) or a Supelco Discovery Bio Wide Pore C18 column (250 × 4.6 mm, 5 μm) using a flow-rate of 1.5 mL/min and detection at 214 nm. Preparative reversed-phase HPLC was performed on either a Kromasil C8 column (250 × 21.2 mm, 5 μm) or a Supelco Discovery Bio Wide Pore C18 column (250 × 21.2 mm, 5 μm) using the same eluent as for the analytical HPLC, a flow-rate of 11 mL/min, and detection at 214 nm. HRMS data were recorded with fast atom bombardment (FAB^+) ionization or electro spray (ES) ionization. *n*-Butyllithium was titrated[84] with diphenyl acetic acid as indicator. Compound **5**,[50] *tert*-butyl glyoxylate,[51] *N*-Fmoc alaninol,[55,56] and $TBDPSO(CH_2)_2CHO$,[62−64] were synthesized as described in the cited literature references. (5*R*)-N^{α}-(Fluoren-9-ylmethoxycarbonyl)-N^{ϵ}-benzyloxycarbonyl-5-*O*-(2,3,4,6-tetra-*O*-acetyl-β-D-galactopyranosyl)-5-hydroxy-L-lysine was prepared according to a published procedure[66] but with some modifications (see Supporting Information). Boc-Gly-Ile-OH was synthesized from commercially available H-Gly-Ile-OH using standard conditions[85] for Boc-protection.

(5*S*)-5-*tert*-Butoxycarbonylamino-4-oxo-hex-2-enoic Acid *tert*-Butyl Ester (6). Lithium chloride (162 mg, 3.82 mmol) and triethylamine (530 μL, 3.80 mmol) were added to a solution of β-ketophosphonate **5**[50] (1.12 g, 3.80 mmol) in MeCN (30 mL) at 0 °C. *tert*-Butyl glyoxylate[51] (705 mg, 5.41 mmol) dissolved in MeCN (34 mL) was added dropwise, and the reaction was stirred for a further 90 min at 0 °C after completed addition. The reaction was quenched by addition of citric acid (10%, aq), Et_2O, and brine, and the organic layer was separated. The aqueous phase was extracted with Et_2O and the combined organic layers were washed with brine, dried, and concentrated under reduced pressure. The residue was purified by flash chromatography (*n*-heptane/EtOAc 8:1 → 2:1) to afford **6** (1.11 g, 97% as an isomeric mixture of *E*/*Z* 3:1) as a slightly yellow oil.

(*E*)-6: ^{1}H NMR ($CDCl_3$) δ 7.08 (d, J = 15.8 Hz, 1H, COCH), 6.74 (d, J = 15.8 Hz, 1H, CHCOO), 5.34−5.21 (m, 1H, NH), 4.61−4.52 (m, 1H, NCH), 1.49 (s, 9H, $C(CH_3)_3$), 1.43 (s, 9H, $C(CH_3)_3$), 1.34 (d, J = 7.1 Hz, 3H, CH_3); ^{13}C NMR ($CDCl_3$) δ 198.4 (CO), 164.3 (COO), 155.1 (NCO), 135.0 (COCH), 134.5 (CHCOO), 82.1 ($C(CH_3)_3$), 80.0 ($C(CH_3)_3$), 54.3 (NCH), 28.3 ($C(CH_3)_3$), 27.9 ($C(CH_3)_3$), 17.6 (CH_3).

(*Z*)-6: ^{1}H NMR ($CDCl_3$) δ 6.46 (d, J = 12.1 Hz, 1H, COCH), 6.04 (d, J = 12.1 Hz, 1H, CHCOO), 5.34−5.21 (m, 1H, NH), 4.50−4.41 (m, 1H, NCH), 1.46 (s, 9H, $C(CH_3)_3$), 1.43 (s, 9H, $C(CH_3)_3$), 1.38 (d, J = 7.2 Hz, 3H, CH_3); ^{13}C NMR ($CDCl_3$) δ 202.1 (CO), 164.6 (COO), 155.1 (NCO), 137.4 (COCH), 128.9 (CHCOO), 82.4 ($C(CH_3)_3$), 79.7 ($C(CH_3)_3$), 55.2 (NCH), 28.3 ($C(CH_3)_3$), 27.9 ($C(CH_3)_3$), 17.3 (CH_3).

(5*S*)-5-*tert*-Butoxycarbonylamino-4-oxo-hexanoic Acid *tert*-Butyl Ester (7). The isomeric mixture of alkenes **6** (133 mg, 0.447 mmol) and Pd/C (15 mg) in EtOAc (15 mL) were stirred under an atmospheric pressure of H_2 for 16 h at rt. The catalyst was removed by filtration through a pad of Celite followed by concentration under reduced pressure and purification by flash chromatography (*n*-heptane/EtOAc 5:1 → 4:1) to afford the saturated analogue **7** (109 mg, 81%) as a colorless oil. $[\alpha]^{20}_D$ +13.3 (*c* 2.0, $CHCl_3$); ^{1}H NMR ($CDCl_3$) δ 5.26 (d, J = 5.8 Hz, 1H, NH), 4.33−4.23 (m, 1H, CH), 2.83−2.72 (m, 1H, $COCH_2$), 2.70−2.62 (m, 1H, $COCH_2$), 2.56−2.41 (m, 2H, CH_2COO), 1.39 (s, 9H, $C(CH_3)_3$), 1.38 (s, 9H, $C(CH_3)_3$), 1.31 (d, J = 7.1 Hz, 3H, CH_3); ^{13}C NMR ($CDCl_3$) δ 208.1 (CO), 171.6 (COO), 155.1 (NCO), 80.6 ($C(CH_3)_3$), 79.6 ($C(CH_3)_3$), 55.0 (CH), 33.8 ($COCH_2$), 28.9 (CH_2COO), 28.2 ($C(CH_3)_3$), 27.9 ($C(CH_3)_3$), 17.7 (CH_3); HRMS (FAB) calcd for $C_{15}H_{28}NO_5$, 302.1967 $[M + H]^+$; found, 302.1980.

(5*S*)-5-(9*H*-Fluoren-9-ylmethoxycarbonylamino)-4-oxo-hexanoic Acid (1). Trifluoroacetic acid (0.7 mL) was added to a stirred solution of **7** (103 mg, 0.342 mmol) in CH_2Cl_2 (3.3 mL) at rt. After 90 min, the solution was concentrated under reduced pressure and the residue was then concentrated from $CHCl_3$ three times. The crude trifluoroacetate salt of **8** was dissolved in H_2O/acetone (1:1, 4 mL), and $NaHCO_3$ (64 mg, 0.762 mmol) was added followed by addition of *N*-(9-fluorenylmethoxycarbonyloxy)succinimide (122 mg, 0.362 mmol). After stirring for 90 min, a second portion of $NaHCO_3$ (32 mg, 0.381 mmol) was added followed by stirring for another 3 h. The acetone was removed under reduced pressure, $CHCl_3$ was added to the aqueous phase and the solution was acidified to pH 2 by addition of HCl (10%, aq) at 0 °C. The organic layer was separated, and the aqueous phase was extracted with $CHCl_3$. The combined organic layers were washed with brine, dried, and concentrated under reduced pressure. Purification by flash chromatography (*n*-heptane/EtOAc/AcOH 3:1:1% → 1:1:1%) afforded **1** (110 mg, 88%) as a white amorphous solid. $[\alpha]^{20}_D$ −15.2 (*c* 1.0, MeOH); ^{1}H NMR (CD_3OD; broad, minor peaks due to the existence of rotamers are not reported) δ 7.79 (d, J = 7.4 Hz, 2H, Fmoc-arom), 7.69−7.63 (m, 2H, Fmoc-arom), 7.41−7.35 (m, 2H, Fmoc-arom), 7.34−7.28 (m, 2H, Fmoc-arom), 4.46 (dd, J = 10.5 and 6.8 Hz, 1H, Fmoc-CH_2), 4.35 (dd, J = 10.5 and 6.8 Hz, 1H, Fmoc-CH_2), 4.24−4.14 (m, 2H, Fmoc-CH, NCH), 2.73 (t, J = 6.1 Hz, 2H, $COCH_2$), 2.56−2.50 (m, 2H, CH_2CO_2H), 1.29 (d, J = 7.2 Hz, 3H, CH_3); ^{13}C NMR (CD_3OD, rotamers) δ 210.7 (CO), 176.2 (CO_2H), 158.4 (NCO), 145.3, 145.2, 142.7, 128.8, 128.2, 128.1, 126.3, 126.1, 120.9, 67.7 (Fmoc-CH_2), 57.0 (NCH), 48.5 (Fmoc-CH), 34.2 ($COCH_2$), 28.5 (CH_2CO_2H), 16.6 (CH_3); HRMS (FAB) calcd for $C_{21}H_{22}NO_5$, 368.1498 $[M + H]^+$; found, 368.1492.

(5*S*)-4-Oxo-5-((2*S*)-3,3,3-trifluoro-2-methoxy-2-phenylpropionylamino)-hexanoic Acid Methyl Ester (9). Compound **7** (41 mg, 0.133 mmol) in CH_2Cl_2 (8.5 mL) was treated with TFA (1.5 mL) for 2 h at rt. The solution was concentrated under reduced pressure, and the residue was then concentrated from $CHCl_3$ four times. The crude product was dissolved in MeOH (2.0 mL), trimethylsilyl chloride (59 μL, 0.465 mmol) was added, and the reaction was stirred for 3 h.[86] The solution was concentrated under reduced pressure and the crude methyl ester was dissolved in CH_2Cl_2 (2.0 mL). (*S*)-(+)-α-Methoxy-α-trifluoromethylphenylacetyl chloride ((*S*)-MTPA-Cl, 30 μL, 0.160 mmol) was added dropwise followed by addition of DIPEA (35 μL, 0.199 mmol), and the reaction was stirred for a further 80 min. The reaction was quenched by addition

of NH_4Cl (1 M, aq), and the phases were separated. The aqueous phase was extracted with CH_2Cl_2, and the combined organic layers were dried and concentrated under reduced pressure to give Mosher amide **9**. The diastereomeric ratio could not be determined from the crude product due to overlapping signals. The crude product was therefore filtered through a silica column with care to minimize any changes in the isomeric ratio. Integration of the ^{1}H NMR spectra displayed a diastereomeric ratio of >100:1.

(5*S*/*R*)-4-Oxo-5-((2*S*)-3,3,3-trifluoro-2-methoxy-2-phenylpropionylamino)-hexanoic Acid Methyl Ester (10). DBU (98 μL, 0.650 mmol) was added to a solution of **7** (15 mg, 0.049 mmol) in THF (1.0 mL) followed by heating at 80 °C for 1800 s by microwave irradiation in a closed vessel. The solution was concentrated under reduced pressure, and the residue was taken up in CH_2Cl_2 and washed with citric acid (10% aq). The combined aqueous phases were extracted with CH_2Cl_2, and the combined organic layers were then washed with brine, dried, and concentrated under reduced pressure to give the crude racemate **rac-7**, $[\alpha]^{20}_D$ 0.0 (*c* 1.0, $CHCl_3$). The corresponding diastereomeric mixture of Mosher amides **10** was synthesized from **rac-7** using the same procedure as described for **9**, and integration of the ^{1}H NMR spectra confirmed a 1:1 diastereomeric mixture.

[(2*S*)-2-(9*H*-Fluoren-9-ylmethoxycarbonylamino)-propylamino]-acetic Acid *tert*-Butyl Ester (14). Dess-Martin periodinane (9.50 mL, 4.57 mmol, 15 wt % solution in CH_2Cl_2) was added to a solution of alcohol **12**[55] (800 mg, 2.69 mmol) in CH_2Cl_2/DMSO (1:1, 24 mL). After stirring for 40 min at rt, the reaction was quenched by addition of $Na_2S_2O_5$ (5.37 g, 28.2 mmol) dissolved in $NaHCO_3$ (aq, satd). The organic layer was separated and washed with $NaHCO_3$ (aq, satd) and H_2O. The combined aqueous phases were extracted with CH_2Cl_2, and the combined organic layers were washed with brine and dried. The solution was concentrated under reduced pressure at low temperature to provide crude aldehyde **13** (643 mg) as a white amorphous solid, which was directly dissolved in CH_2Cl_2 (15 mL) and treated with glycine *tert*-butyl ester hydrochloride (438 mg, 2.61 mmol) at rt for 40 min. $NaBH(OAc)_3$ (738 mg, 3.48 mmol) and MeOH (3.6 mL) were added to the reaction. After 90 min, $NaHCO_3$ (aq, satd) and brine were added, the organic layer was separated, and the aqueous phase was extracted with CH_2Cl_2. The combined organic layers were dried and concentrated under reduced pressure. Purification by flash chromatography (silica gel pretreated with AcOH, *n*-heptane/EtOAc/triethylamine 2:3:0% → 1:4:2%) afforded secondary amine **14** (468 mg, 43% from **12**) as a slightly yellow oil. $[\alpha]^{20}_D$ +2.1 (*c* 1.0, $CHCl_3$); ^{1}H NMR ($CDCl_3$) δ 7.76 (d, J = 7.5 Hz, 2H, Fmoc-arom), 7.64−7.59 (m, 2H, Fmoc-arom), 7.42−7.37 (m, 2H, Fmoc-arom), 7.34−7.29 (m, 2H, Fmoc-arom), 5.25 (br s, 1H, CONH), 4.39 (d, J = 6.9 Hz, 2H, Fmoc-CH_2), 4.23 (t, J = 6.9 Hz, 1H, Fmoc-CH), 3.86−3.74 (m, 1H, NCH), 3.38−3.22 (m, 2H, $COCH_2$), 2.70−2.61 (m, 2H, NCH_2CH), 1.96 (br s, 1H, NH), 1.48 (s, 9H, $C(CH_3)_3$), 1.22−1.14 (m, 3H, CH_3); ^{13}C NMR ($CDCl_3$, rotamers) δ 171.7 (COO), 156.1 (NCO), 144.0, 144.0, 141.3, 127.6, 127.0, 125.1, 119.9, 81.3 ($C(CH_3)_3$), 66.5 (Fmoc-CH_2), 54.2 (NCH_2CH), 51.6 ($COCH_2$), 47.3 (NCH), 46.8 (Fmoc-CH), 28.1 ($C(CH_3)_3$), 18.9 (CH_3); HRMS (FAB) calcd for $C_{24}H_{31}N_2O_4$, 411.2284 $[M + H]^+$; found, 411.2275.

{*tert*-Butoxycarbonyl-[(2*S*)-2-(9*H*-fluoren-9-ylmethoxycarbonylamino)-propyl]-amino}-acetic Acid (2). Secondary amine **14** (255 mg, 0.621 mmol) was dissolved in CH_2Cl_2 (20 mL) and treated with trifluoroacetic acid (8.6 mL). The reaction was stirred for 14 h at rt followed by concentration under reduced pressure. The residue was concentrated from $CHCl_3$ three times and was then dissolved in CH_2Cl_2 (12 mL). Diisopropylethylamine (238 μL, 1.37 mmol) was added followed by addition of Boc_2O (186 mg, 0.853 mmol) dissolved in CH_2Cl_2 (2.0 mL). After 40 min, a second portion of DIPEA (66 μL, 0.379 mmol) and Boc_2O (177 mg, 0.811 mmol) were added. After an additional 15 min, the reaction was quenched by addition of citric acid (10%, aq), the phases were separated, and the aqueous phase was extracted with CH_2Cl_2. The combined organic layers were washed with brine, dried, and concentrated under reduced pressure. The residue was purified by flash chromatography (*n*-heptane/EtOAc/AcOH 3:1:2% → 2:1:2%) to give carboxylic acid **2** (252 mg, 89%) as a white foam. $[\alpha]^{20}_D$ −5.1 (*c* 1.0, $CHCl_3$); ^{1}H NMR ($CDCl_3$, rotamers) δ 7.75 (d, J = 7.5 Hz, 2H, Fmoc-arom), 7.61−7.54 (m, 2H, Fmoc-arom), 7.41−7.36 (m, 2H, Fmoc-arom), 7.33−7.26 (m, 2H, Fmoc-arom), 5.55 (d, J = 6.6 Hz, 0.6H, NH), 5.11−5.02 (m, 0.4H, NH), 4.41 (d, J = 5.1 Hz, 0.8H, Fmoc-CH_2), 4.32 (d, J = 6.8 Hz, 1.2H, Fmoc-CH_2), 4.22−4.14 (m, 1H, Fmoc-CH), 4.01−3.91 (m, 2H, CH_2CO_2H), 3.91−3.80 (m, 0.8H, NCH), 3.70−3.58 (m, 0.7H, $CHCH_2$), 3.58−3.46 (m, 0.2H, NCH), 3.44−3.33 (m, 0.3H, $CHCH_2$), 3.26−3.15 (m, 0.4H, $CHCH_2$), 3.11−2.98 (m, 0.6H, $CHCH_2$), 1.44 (s, 3.2H, $C(CH_3)_3$), 1.41 (s, 5.8H, $C(CH_3)_3$), 1.21−1.14 (m, 2.5H, CH_3), 1.08−0.93 (m, 0.5H, CH_3); ^{13}C NMR ($CDCl_3$, rotamers [δ for minor rotamer when assigned]) δ 174.2 [173.9] (CO_2H), 156.5 (NCOO), 156.3 (NCOO), 155.9 (NCOO), 143.9, 143.8, 141.3, 141.2, 127.6, 127.0, 125.2, 124.9, 119.9, 119.9, 81.2 [81.5] ($C(CH_3)_3$), 66.8 [66.5] (Fmoc-CH_2), 52.8 [53.3] ($CHCH_2$), 49.8 (CH_2CO_2H), 47.2 (Fmoc-CH), 46.9 [46.7] (NCH), 28.1 [28.2] ($C(CH_3)_3$), 18.6 (CH_3); HRMS (FAB) calcd for $C_{25}H_{31}N_2O_6$, 455.2182 $[M + H]^+$; found, 455.2189.

***N*-Trifluoroacetyl-(2*S*)-alaninol (17).** L-Alaninol (2.50 g, 33.3 mmol) dissolved in CH_2Cl_2 (200 mL) was treated with triethylamine (16.3 mL, 117 mmol) at rt. The solution was cooled to 0 °C, trifluoroacetic anhydride (6.5 mL, 46.6 mmol) was slowly added over 40 min, and the reaction was stirred for 6 h after complete addition. The solution was concentrated under reduced pressure at low temperature and the crude product was dissolved in EtOAc and washed with $NaHCO_3$ (aq, satd). The aqueous phase was extracted with EtOAc, and the combined organic layers were washed with HCl (0.1 M, aq) and brine. The organic layer was dried and concentrated under reduced pressure to afford alcohol **17** (4.43 g, 78%) as a white amorphous solid, which was used without further purification. $[\alpha]^{20}_D$ −16.3 (*c* 1.0, $CHCl_3$); ^{1}H NMR ($CDCl_3$) δ 6.77 (br s, 1H, NH), 4.17−4.06 (m, 1H, CH), 3.74 (dd, J = 11.2 and 3.8 Hz, 1H, CH_2), 3.61 (dd, J = 11.2 and 4.9 Hz, 1H, CH_2), 2.38 (br s, 1H, OH), 1.26 (d, J = 6.9 Hz, 3H, CH_3); ^{13}C NMR ($CDCl_3$) δ 157.1 (q, J_{C-F} = 37 Hz, NCO), 115.8 (q, J_{C-F} = 287 Hz, CF_3), 65.0 (splitted, CH_2), 47.8 (splitted, CH), 16.5 (splitted, CH_3); HRMS (ES) calcd for $C_5H_9F_3NO_2$, 172.0585 $[M + H]^+$; found, 172.0570.

***N*-((1*S*)-2-Iodo-1-methyl-ethyl)-trifluoroacetamide (18).** Triphenylphosphine (7.51 g, 28.6 mmol) and imidazole (2.20 g, 32.3 mmol) were added to alcohol **17** (2.04 g, 11.9 mmol) dissolved in toluene (140 mL). The solution was treated with I_2 (5.80 g, 22.9 mmol) and was slightly heated during addition. After 75 min, Et_2O was added, and the organic phase was washed with $Na_2S_2O_3$ (5%, aq). The aqueous phase was extracted with Et_2O, and the combined organic layers were dried and concentrated under reduced pressure. The residue was purified by flash chromatography (*n*-heptane/EtOAc 40:1 → 2:1) to afford iodide **18** (2.64 g, 79%) as a white amorphous solid. $[\alpha]^{20}_D$ −47.2 (*c* 1.0, $CHCl_3$); ^{1}H NMR ($CDCl_3$) δ 6.56 (br s, 1H, NH), 3.96−3.85 (m, 1H, CH), 3.43 (dd, J = 10.5 and 4.9 Hz, 1H, CH_2), 3.29 (dd, J = 10.5 and 4.5 Hz, 1H, CH_2), 1.32 (d, J = 6.7 Hz, 3H, CH_3); ^{13}C NMR ($CDCl_3$) δ 156.5 (q, J_{C-F} = 37 Hz, NCO), 115.6 (q, J_{C-F} = 288 Hz, CF_3), 45.8 (CH), 20.5 (CH_3), 12.0 (CH_2); HRMS (ES) calcd for $C_5H_8F_3INO$, 281.9603 $[M + H]^+$; found, 281.9621.

((2*S*)-2-Trifluoroacetamido-propyl)-triphenyl Phosphonium Iodide (19). Iodide **18** (1.76 g, 6.26 mmol) and PPh_3 (6.63 g, 25.3 mmol) were refluxed in toluene (22 mL) for 18 h. The solvent was evaporated under reduced pressure and the residue was purified by flash chromatography (CH_2Cl_2/MeOH 1:0 → 30:1) to give phosphonium salt **19** (3.40 g, quantitative yield) as a white foam. $[\alpha]^{20}_D$ −17.2 (*c* 1.0, $CHCl_3$); ^{1}H NMR (CD_3OD) δ 7.93−7.85 (m, 8H, Ph), 7.80−7.73 (m, 6H, Ph), 4.65−4.53 (m, 1H, CH), 4.03−3.82 (m, 2H, CH_2), 1.47 (dd, J = 6.6 and 1.9 Hz, 3H, CH_3); ^{13}C NMR (CD_3OD) δ 157.5 (q, J_{C-F} = 37 Hz, NCO), 136.3 (d, J_{C-P} = 2.9 Hz, Ph), 134.9 (d, J_{C-P} = 10 Hz, Ph), 131.5 (d, J_{C-P} = 13 Hz, Ph), 119.1 (d, J_{C-P} = 108 Hz, Ph), 116.6 (q, J_{C-F} = 288 Hz, CF_3), 42.6 (d, J_{C-P} = 4.4 Hz, CH), 29.2 (d, J_{C-P} = 51 Hz, CH_2),

23.5 (d, J_{C-P} = 14 Hz, CH_3); HRMS (FAB) calcd for $C_{23}H_{22}F_3NOP$, 416.1386 $[M]^+$; found, 416.1400.

***N*-[(1*S*)-5-(*tert*-Butyl-diphenyl-silyloxy)-1-methyl-pent-2-enyl]-trifluoroacetamide (20).** Phosphonium salt **19** (1.46 g, 2.94 mmol) was dried under vacuum overnight before being dissolved in THF (25 mL) and cooled to −78 °C. Titrated[84] *n*-BuLi (4.20 mL, 1.4 M in hexanes, 5.88 mmol) was slowly added whereby the solution turned bright yellow. The reaction was allowed to reach rt during 20 min and was then cooled to −78 °C again followed by addition of 3-(*tert*-butyl-diphenyl-silyloxy)-propionaldehyde[62−64] ($TBDPSO(CH_2)_2$-CHO, 919 mg, 2.94 mmol) dissolved in THF (8 mL). The reaction was allowed to reach 0 °C over a period of 110 min, followed by addition of Et_2O and 0.1 M HCl saturated with NH_4Cl. The organic layer was separated and the aqueous phase was extracted with Et_2O. The combined organic layers were washed with brine, dried, and concentrated under reduced pressure. The residue was purified by flash chromatography (*n*-heptane/EtOAc 10:1 → 8:1) to afford **20** (1.17 g, 89%) as an isomeric mixture of *E*/*Z* 1:1 (this reaction typically gave mixtures of alkenes of *E*/*Z* 3:2−2:3). ^1H NMR ($CDCl_3$, *E*/*Z* isomers) δ 7.69−7.63 (m, 8H, Ph), 7.45−7.35 (m, 12H, Ph), 6.18 (br s, 1H, NH_Z), 6.12 (br s, 1H, NH_E), 5.74−5.66 (m, 1H, NCHCHCH_E), 5.66−5.58 (m, 1H, NCHCHCH_Z), 5.48 (dd, J = 16.4 and 5.9 Hz, 1H, NCHCH_E), 5.40−5.31 (m, 1H, NCHCH_Z), 4.82−4.71 (m, 1H, NCH_Z), 4.60−4.50 (m, 1H, NCH_E), 3.77−3.63 (m, 4H, CH_2OSi), 2.49−2.34 (m, 2H, C$H_2CH_2OSi_Z$), 2.33−2.25 (m, 2H, C$H_2CH_2OSi_E$), 1.30 (d, J = 6.8 Hz, 3H, $CH_{3\ E}$), 1.26 (d, J = 6.7 Hz, 3H, $CH_{3\ Z}$), 1.06 (s, 18H, $C(CH_3)_3$); ^{13}C NMR ($CDCl_3$, *E*/*Z* isomers) δ 156.1 (q, J_{C-F} = 37 Hz, NCO), 156.0 (q, J_{C-F} = 37 Hz, NCO), 135.5 (Ph), 134.8 (Ph), 133.8 (Ph), 133.8 (Ph), 133.7 (Ph), 130.9 (NCH*C*H_E), 130.5 (NCHCH*C*H_Z), 130.3 (NCH*C*H_Z), 129.6 (Ph), 129.6 (Ph), 129.5 (NCHCH*C*H_E), 127.6 (Ph), 115.8 (q, J_{C-F} = 288 Hz, CF_3), 115.8 (q, J_{C-F} = 288 Hz, CF_3), 63.1 (CH_2OSi), 63.1 (CH_2OSi), 47.4 (NCH_E), 43.9 (NCH_Z), 35.5 (*C*H_2-CH_2OSi_E), 31.1 (*C*$H_2CH_2OSi_Z$), 26.8 ($C(CH_3)_3$), 26.8 ($C(CH_3)_3$), 21.1 ($CH_{3\ Z}$), 20.1 ($CH_{3\ E}$), 19.2 ($C(CH_3)_3$), 19.2 ($C(CH_3)_3$).

(5*S*)-5-(Trifluoroacetamido)-hex-3-en-1-ol (21). The isomeric mixture of **20** (1.10 g, 2.46 mmol, *E*/*Z* 1:1) in THF (50 mL) was treated with tetrabutylammonium fluoride trihydrate (2.33 g, 7.37 mmol) for 6 h at rt. The solvent was evaporated under reduced pressure and the residue was purified by flash chromatography (*n*-heptane/EtOAc 4:1 → 2:1) twice to completely separate **(*E*)-21** (148 mg, 29%) and **(*Z*)-21** (156 mg, 30%).

(*E*)-21: A colorless oil; $[\alpha]^{20}_D$ −75.6 (*c* 1.0, $CHCl_3$); ^1H NMR ($CDCl_3$) δ 6.90−6.80 (m, 1H, NH), 5.68−5.59 (m, 1H, C*H*CH_2), 5.51 (dd, J = 15.6 and 5.9 Hz, 1H, NCHC*H*), 4.56−4.46 (m, 1H, NCH), 3.64 (t, J = 6.2 Hz, 2H, CH_2OH), 2.37 (br s, 1H, OH), 2.30−2.24 (m, 2H, CH_2CH_2OH), 1.30 (d, J = 6.9 Hz, 3H, CH_3); ^{13}C NMR ($CDCl_3$) δ 156.5 (q, J_{C-F} = 37 Hz, NCO), 131.9 (NCH*C*H), 128.8 (*C*HCH_2), 115.8 (q, J_{C-F} = 288 Hz, CF_3), 61.4 (CH_2OH), 47.6 (NCH), 35.4 (*C*H_2CH_2OH), 20.0 (CH_3); HRMS (FAB) calcd for $C_8H_{13}F_3NO_2$, 212.0898 $[M + H]^+$; found, 212.0887.

(*Z*)-21: A colorless oil; $[\alpha]^{20}_D$ −12.4 (*c* 1.0, $CHCl_3$) ^1H NMR ($CDCl_3$) δ 6.73 (br s, 1H, NH), 5.61−5.53 (m, 1H, C*H*CH_2CH_2-OH), 5.45−5.39 (m, 1H, NCHC*H*), 4.82−4.71 (m, 1H, NCH), 3.75−3.61 (m, 2H, CH_2OH), 2.55−2.45 (m, 1H, CH_2CH_2OH), 2.36−2.27 (m, 1H, CH_2CH_2OH), 2.23 (br s, 1H, OH), 1.31 (d, J = 6.7 Hz, 3H, CH_3); ^{13}C NMR ($CDCl_3$) δ 156.5 (q, J_{C-F} = 37 Hz, NCO), 131.6 (NCH*C*H), 129.8 (*C*HCH_2), 115.7 (q, J_{C-F} = 288 Hz, CF_3), 61.5 (*C*H_2OH), 44.0 (NCH), 31.0 (*C*H_2CH_2OH), 20.8 (CH_3); HRMS (FAB) calcd for $C_8H_{13}F_3NO_2$, 212.0898 $[M + H]^+$; found, 212.0888.

General Procedure for Oxidation of (*E*)-21 and (*Z*)-21 to Afford 22 and 24. Jones' reagent (1 M CrO_3 (3.0 equiv) in 4.4 M H_2SO_4) was added to alcohol **(*E*)-21** or **(*Z*)-21** (1.0 equiv) dissolved in acetone (20.5 mL/mmol alcohol) at 0 °C, and the solution was stirred for 45 min, while allowed to attain rt. *i*-PrOH (1 mL) was added, and the pH was adjusted to 3 by addition of $NaHCO_3$ (aq, satd). The aqueous phase was extracted with Et_2O, and the combined organic layers were dried and concentrated under reduced pressure.

(*E*)-(5*S*)-5-(Trifluoroacetamido)-hex-3-enoic Acid (22). The general procedure described above applied on **(*E*)-21** (134 mg, 0.635 mmol) in acetone (13 mL) followed by flash chromatography (*n*-heptane/EtOAc/AcOH 4:1:1% → 3:1:1%) afforded carboxylic acid **22** (132 mg, 92%) as a white amorphous solid. $[\alpha]^{20}_D$ −72.0 (*c* 1.0, $CHCl_3$); ^1H NMR ($CDCl_3$) δ 6.35−6.23 (m, 1H, NH), 5.82−5.73 (m, 1H, C*H*CH_2CO_2H), 5.62 (dd, J = 15.6 and 5.7 Hz, 1H, NCHC*H*), 4.65−4.55 (m, 1H, NCH), 3.14 (d, J = 6.8 Hz, 2H, CH_2-CO_2H), 1.35 (d, J = 6.9 Hz, 3H, CH_3); ^{13}C NMR ($CDCl_3$) δ 176.6 (CO_2H), 156.3 (J_{C-F} = 37 Hz, NCO), 133.6 (NCH*C*H), 123.4 (*C*HCH_2CO_2H), 115.8 (J_{C-F} = 288 Hz, CF_3), 47.1 (NCH), 37.0 (*C*H_2CO_2H), 19.9 (CH_3); HRMS (FAB) calcd for $C_8H_{11}F_3NO_3$, 226.0691 $[M + H]^+$; found, 226.0689.

(*Z*)-(5*S*)-5-(Trifluoroacetamido)-hex-3-enoic Acid (24). The general procedure described above applied on **(*Z*)-21** (144 mg, 0.682 mmol) in acetone (14 mL) followed by flash chromatography (*n*-heptane/EtOAc/AcOH 4:1:1%) afforded carboxylic acid **24** (133 mg, 87%) as a colorless oil. $[\alpha]^{20}_D$ +13.3 (*c* 1.0, $CHCl_3$); ^1H NMR ($CDCl_3$) δ 10.8 (br s, 1H, CO_2H), 6.44 (br s, 1H, NH), 5.77−5.69 (m, 1H, C*H*CH_2CO_2H), 5.54−5.46 (m, 1H, NCHC*H*), 4.80−4.69 (m, 1H, NCH), 3.29 (dd, J = 7.4 and 1.6 Hz, 2H, CH_2CO_2H), 1.33 (d, J = 6.7 Hz, 3H, CH_3); ^{13}C NMR ($CDCl_3$) δ 176.7 (CO_2H), 156.4 (J_{C-F} = 37 Hz, NCO), 132.7 (NCH*C*H), 124.2 (*C*HCH_2-CO_2H), 115.7 (J_{C-F} = 288 Hz, CF_3), 43.7 (NCH), 32.9 (*C*H_2CO_2H), 20.6 (CH_3); HRMS (FAB) calcd for $C_8H_{11}F_3NO_3$, 226.0691 $[M + H]^+$; found, 226.0701.

General Procedure for Hydrolysis of 22 and 24 and Subsequent Fmoc-Protection to Afford 3 and 26. Trifluoroacetamide **22** or **24** (1.0 equiv) was dissolved in MeOH (19 mL/mmol trifluoroacetamide), and K_2CO_3 (10% aq, 7.5 mL/mmol trifluoroacetamide) was added followed by stirring for 19−36 h at rt. The solvent was removed under reduced pressure, and the residue was dissolved in Na_2CO_3 (10%, aq)/MeCN (1:1, 29 mL/mmol), followed by addition of *N*-(9-fluorenylmethoxycarbonyloxy)succinimide (1.05 equiv). After stirring for 8−16 h, the MeCN was evaporated under reduced pressure, $CHCl_3$ was added, and the aqueous phase was acidified to pH 2 by addition of HCl (10% aq) at 0 °C. The organic layer was separated, and the aqueous phase was extracted with $CHCl_3$. The combined organic layers were washed with brine, dried, and concentrated under reduced pressure, followed by purification by flash chromatography (*n*-heptane/EtOAc/AcOH 3:1:1%).

(*E*)-(5*S*)-5-(9*H*-Fluoren-9-ylmethoxycarbonylamino)-hex-3-enoic Acid (3). The general procedure described above applied on **22** (122 mg, 0.543 mmol) afforded the Fmoc-protected building block **3** (169 mg, 89%) as a white amorphous solid. $[\alpha]^{20}_D$ −18.8 (*c* 1.0, MeOH); ^1H NMR ($CDCl_3$) δ 7.76 (d, J = 7.6 Hz, 2H, Fmoc-arom), 7.59 (d, J = 7.4 Hz, 2H, Fmoc-arom), 7.42−7.37 (m, 2H, Fmoc-arom), 7.34−7.29 (m, 2H, Fmoc-arom), 5.75−5.49 (m, 2H, NCHC*H*, C*H*CH_2CO_2H), 4.92 (br s, 1H, NH), 4.50−4.38 (m, 2H, Fmoc-CH_2), 4.35−4.25 (m, 1H, NCH), 4.22 (t, J = 6.5 Hz, 1H, Fmoc-CH), 3.15−3.04 (m, 2H, CH_2CO_2H), 1.34−1.12 (m, 3H, CH_3); ^{13}C NMR ($CDCl_3$) δ 176.4 (CO_2H), 155.6 (NCO), 143.9, 141.4, 135.9 (NCH*C*H), 127.7, 127.0, 125.0, 121.5 (*C*HCH_2CO_2H), 120.0, 66.6 (Fmoc-CH_2), 48.0 (NCH), 47.3 (Fmoc-CH), 37.1 (*C*H_2-CO_2H), 20.8 (CH_3); HRMS (FAB) calcd for $C_{21}H_{22}NO_4$, 352.1549 $[M + H]^+$; found, 352.1552.

(*Z*)-(5*S*)-5-(9*H*-Fluoren-9-ylmethoxycarbonylamino)-hex-3-enoic Acid (26). The general procedure described above applied on **24** (100 mg, 0.445 mmol) afforded the Fmoc-protected building block **26** (134 mg, 86%) as a white amorphous solid. $[\alpha]^{20}_D$ +71.2 (*c* 1.0, MeOH); ^1H NMR ($CDCl_3$) δ 7.76 (d, J = 7.6 Hz, 2H, Fmoc-arom), 7.57 (d, J = 7.6 Hz, 2H, Fmoc-arom), 7.42−7.37 (m, 2H, Fmoc-arom), 7.31 (m, 2H, Fmoc-arom), 5.67−5.56 (m, 1H, C*H*CH_2-CO_2H), 5.46−5.38 (m, 1H, NCHC*H*), 4.79 (br s, 1H, NH), 4.52−4.37 (m, 3H, Fmoc-CH_2, NCH), 4.20 (t, J = 6.3 Hz, 1H, Fmoc-CH), 3.45−3.31 (m, 1H, CH_2CO_2H), 3.27−3.14 (m, 1H, CH_2CO_2H), 1.30−1.16 (m, 3H, CH_3); ^{13}C NMR ($CDCl_3$, rotamers) δ 174.6 (CO_2H), 155.9 (NCO), 143.8, 143.8, 141.3, 134.9 (NCH*C*H), 127.7, 127.1, 124.9, 124.9, 122.4 (*C*HCH_2CO_2H), 120.0, 66.8 (Fmoc-CH_2),

Table 2. ^{1}H NMR Chemical Shifts for CII260−267 with GalHyl^{264} and Ala$^{261}\psi$[$COCH_2$]Gly^{262} (**28**)[a]

residue	NH	Hα	Hβ	Hγ	others
Ile^{260}	8.08	4.11	1.81	1.45, 1.18, 0.91 (CH_3)	0.86 (Hδ)[b]
Ala$^{261}\psi$[$COCH_2$]	8.42	4.40	1.29		2.83 and 2.75 ($COCH_2$)
Gly^{262}		2.46[c]			
Phe^{263}	8.21	4.57	3.07, 3.01		7.25 (Hδ), 7.34 (Hε), 7.31 (Hζ)
Hyl^{264}	8.35	4.26	2.00, 1.73	1.59[c]	4.01 (Hδ), 3.17 and 2.97 (Hε)[d]
Gly^{265}	7.91	3.88[c]			
Glu^{266}	8.26	4.31	2.08, 1.93	2.41[c]	
Gln^{267}	8.44	4.26	2.08, 1.96	2.34[c]	7.47 and 6.82 (δNH_2)[e]

[a] Measured at 500 MHz and 298 K in water containing 10% D_2O with H_2O (δ_H 4.76 ppm) as internal standard. [b] Chemical shift for the N-terminal acetate group: δ 2.01. [c] Degeneracy has been assumed. [d] Chemical shifts for the galactose moiety: δ 4.42 (H1), 3.91 (H4), 3.75 (H6), 3.68 (H5), 3.63 (H3), and 3.52 (H2). [e] Chemical shifts for the C-terminal amide: δ 7.55, 7.08.

Table 3. ^{1}H NMR Chemical Shifts for CII260−267 with GalHyl^{264} and Ala$^{261}\psi$[$CH_2NH_2^+$]Gly^{262} (**29**)[a]

residue	NH	Hα	Hβ	Hγ	others
Ile^{260}	8.13	4.07	1.87	1.18, 1.42, 0.90 (CH_3)	0.86 (Hδ)[b]
Ala$^{261}\psi$[$CH_2NH_2^+$]	8.12	4.20	1.22		3.08 and 3.00 ($CH_2NH_2^+$)
Gly^{262}		3.86[c]			
Phe^{263}	8.56	4.72	3.11, 2.99		7.26 (Hδ), 7.34 (Hε), 7.31 (Hζ)
Hyl^{264}	8.52	4.26	1.99, 1.76	1.60[c]	4.01 (Hδ), 3.16 and 2.97 (Hε)[d]
Gly^{265}	8.13	3.90[c]			
Glu^{266}	8.21	4.31	2.07, 1.88	2.43[c]	
Gln^{267}	8.47	4.26	2.08, 1.97	2.33[c]	7.48 and 6.82 (δNH_2)[e]

[a] Measured at 500 MHz and 298 K in water containing 10% D_2O with H_2O (δ_H 4.76 ppm) as internal standard. [b] Chemical shift for the N-terminal acetate group: δ 2.03. [c] Degeneracy has been assumed. [d] Chemical shifts for the galactose moiety: δ 4.43 (H1), 3.91 (H4), 3.76 (H6), 3.69 (H5), 3.64 (H3), and 3.53 (H2). [e] Chemical shifts for the C-terminal amide: δ 7.57, 7.09.

Table 4. ^{1}H NMR Chemical Shifts for CII259−273 with GalHyl^{264} and Ala$^{261}\psi$[$COCH_2$]Gly^{262} (**31**)[a]

residue	NH	Hα	Hβ	Hγ	others
Gly^{259}		3.84[b]			
Ile^{260}	8.44	4.21	1.82	1.44, 1.17, 0.92 (CH_3)	0.85 (Hδ)
Ala$^{261}\psi$[$COCH_2$]	8.53	4.42	1.30		2.84 and 2.74 ($COCH_2$)
Gly^{262}		2.47[b]			
Phe^{263}	8.18	4.59	3.06, 3.00		7.24 (Hδ), 7.33 (Hε), 7.31 (Hζ)
Hyl^{264}	8.35	4.26	1.99, 1.73	1.59[b]	4.00 (Hδ), 3.16 and 2.98 (Hε)[c]
Gly^{265}	7.97	3.88[b]			
Glu^{266}	8.19	4.35	2.11, 1.94	2.44[b]	
Gln^{267}	8.48	4.36	2.10, 1.96	2.35[b]	7.48 and 6.81 (δNH_2)
Gly^{268}	8.26	4.11, 3.98			
Pro^{269}		4.40	2.26, 1.90	1.98[b]	3.58[b] (Hδ)
Lys^{270}	8.44	4.28	1.82, 1.74	1.44[b]	1.66[b] (Hδ), 2.97[b] (Hε)
Gly^{271}	8.34	3.93[b]			
Glu^{272}	8.20	4.46	2.14, 1.96	2.45[b]	
Thr^{273}	8.10	4.33	4.33	1.16	

[a] Measured at 500 MHz and 298 K in water containing 10% D_2O with H_2O (δ_H 4.76 ppm) as internal standard. The glycopeptide existed in two forms in solution due to *cis*/*trans* isomerization of the Gly^{268}−Pro^{269} amide bond. Shifts are reported for the major *trans*-isomer (displayed NOEs between Gly^{268} H^{α} and Pro^{269} $H^{\delta,\delta'}$), while the minor *cis*-isomer (<15%) could not be completely assigned due to spectral overlap. [b] Degeneracy has been assumed. [c] Chemical shifts for the galactose moiety: δ 4.42 (H1), 3.90 (H4), 3.75 (H6), 3.67 (H5), 3.62 (H3), and 3.51 (H2).

47.3 (Fmoc-CH), 44.3 (NCH), 33.6 (CH_2CO_2H), 21.0 (CH_3); HRMS (FAB) calcd for $C_{21}H_{22}NO_4$, 352.1549 $[M + H]^+$; found, 352.1545.

General Procedure for Solid-Phase Glycopeptide Synthesis. All glycopeptides were synthesized in mechanically agitated reactors using standard solid-phase methodology according to the Fmoc-protocol essentially as described elsewhere.[19] Glycopeptides **31**, **32**, **33**, and **34** were synthesized on Tentagel-S-PHB-Thr-Fmoc resins, whereas **28** and **29** were synthesized as C-terminal amides on Tentagel-S-NH_2 resins by first coupling the linker Fmoc-2,4-dimethoxy-4′-(carboxymethyloxy)-benzhydrylamine (Rink). All couplings were performed in DMF, unless otherwise stated, and monitored either by using bromophenol blue as indicator[87] or by performing a Kaiser test.[88] N^{α}-Fmoc amino acids (4 equiv) with standard side chain protecting groups and the Rink linker (4 equiv) were activated with 1-hydroxy-benzotriazole (HOBt, 6 equiv) and diisopropyl carbodiimide (DIC, 3.9 equiv). (5*R*)-N^{α}-(Fluoren-9-ylmethoxycarbonyl)-N^{ϵ}-benzyloxycarbonyl-5-*O*-(2,3,4,6-*tetra*-*O*-acetyl-β-D-galactopyranosyl)-5-hydroxy-L-lysine[66] (1.5−1.6 equiv) was coupled for 24−37 h using 1-hydroxy-7-azabenzotriazole (HOAt, 3.0−3.4 equiv) and DIC (1.5−1.6 equiv) as coupling reagents. Isostere building blocks **1**, **2**, **3**, and **26** (1.5−1.8 equiv) were coupled for 26−46 h using *O*-(7-azabenzotriazol-1-yl)-1,1,3,3-tetramethyluronium hexafluorophosphate (HATU, 1.6−2.2 equiv) and 2,4,6-collidine (3.2−3.5 equiv), except in the synthesis of **28**, where building block **1** (2.0 equiv) was instead activated with HOAt (4.7 equiv) and DIC (2.1 equiv). Fmoc-deprotection after each coupling cycle was accomplished by treatment with 20% piperidine in DMF for 10 min. Cleavage of the glycopeptides from the solid phase by treatment with trifluoroacetic acid/H_2O/thioanisole/ethanedithiol (35:2:2:1) at 40 °C for 3 h and subsequent workup was performed essentially as described elsewhere.[19] This was followed by purification by reversed-phase HPLC using a 0−100% linear gradient of MeCN (0.1% TFA) in H_2O (0.1% TFA) over 60 min, except in the synthesis of **29**, where the crude acetylated glycopeptide was directly deacetylated. Deacetylation was accomplished by treatment with NaOMe in MeOH (20 mM, 1 mL/mg peptide) for 2−3 h. Neutralization by addition of AcOH and concentration under reduced pressure was followed by purification using reversed-phase HPLC and the same eluent as stated previously.

Ac-L-isoleucyl-L-alanylψ[$COCH_2$]glycyl-L-phenylalanyl-5-*O*-(β-D-galactopyranosyl)-5-hydroxy-L-lysylglycyl-L-glutam-1-yl-L-glutamine (28). Synthesis was performed with building block **1**

Table 5. ^{1}H NMR Chemical Shifts for CII259−273 with GalHyl^{264} and Ala$^{261}\psi$[$CH_2NH_2^+$]Gly^{262} (**32**)[a]

residue	NH	Hα	Hβ	Hγ	others
Gly^{259}		3.87[b]			
Ile^{260}	8.50	4.16	1.87	1.41, 1.16, 0.90 (CH_3)	0.85 (Hδ)
Ala$^{261}\psi$[$CH_2NH_2^+$]	8.27	4.18	1.23		3.10 and 2.98 ($CH_2NH_2^+$)
Gly^{262}		3.91, 3.84			
Phe^{263}	8.56	4.72	3.13, 3.00		7.24 (Hδ), 7.33 (εH), 7.31 (Hζ)
Hyl^{264}	8.52	4.28	2.00, 1.80	1.61[b]	4.03 (Hδ), 3.12 and 2.99 (Hε)[c]
Gly^{265}	8.17	3.96, 3.87			
Glu^{266}	8.18	4.33	2.06, 1.87	2.40[b]	
Gln^{267}	8.50	4.37	2.12, 1.88	2.36[b]	7.49 and 6.82 (δNH_2)
Gly^{268}	8.27	4.11, 3.98			
Pro^{269}		4.39	2.26, 1.90	1.98[b]	3.58[b]
Lys^{270}	8.44	4.29	1.84, 1.76	1.45[b]	1.67[b] (Hδ), 2.99[b] (Hε)
Gly^{271}	8.34	3.94[b]			
Glu^{272}	8.19	4.46	2.16, 1.97	2.45[b]	
Thr^{273}	8.04	4.30	4.30	1.16	

[a] Measured at 500 MHz and 298 K in water containing 10% D_2O with H_2O (δ_H 4.76 ppm) as internal standard. The glycopeptide existed in two forms in solution due to *cis*/*trans* isomerization of the Gly^{268}−Pro^{269} amide bond. Shifts are reported for the major *trans*-isomer (displayed NOEs between Gly^{268} H$^{\alpha}$ and Pro^{269} H$^{\delta,\delta'}$), while the minor *cis*-isomer (<15%) could not be completely assigned due to spectral overlap. [b] Degeneracy has been assumed. [c] Chemical shifts for the galactose moiety: δ 4.42 (H1), 3.91 (H4), 3.76 (H6), 3.68 (H5), 3.63 (H3), and 3.52 (H2).

Table 6. ^{1}H NMR Chemical Shifts for CII259−273 with GalHyl^{264} and Ala$^{261}\psi$[(*E*)-CH═CH]Gly^{262} (**33**)[a]

residue	NH	Hα	Hβ	Hγ	others
Gly^{259}		3.84[b]			
Ile^{260}	8.39	4.11	1.78	1.43, 1.14, 0.87 (CH_3)	0.82 (Hδ)
Ala$^{261}\psi$[(*E*)-CH═CH]	8.24	4.36	1.19		5.51[b] (CH═CH)
Gly^{262}		2.95[b]			
Phe^{263}	8.07	4.59	3.08, 2.98		7.22 (Hδ), 7.33 (Hε), 7.29 (Hζ)
Hyl^{264}	8.42	4.27	2.01, 1.75	1.61[b]	4.02 (Hδ), 3.07 and 2.97 (Hε)[c]
Gly^{265}	7.99	3.92, 3.86			
Glu^{266}	8.21	4.36	2.09, 1.93	2.44[b]	
Gln^{267}	8.48	4.37	2.11, 1.97	2.35[b]	7.48 and 6.81 (δNH_2)
Gly^{268}	8.26	4.12, 3.98			
Pro^{269}		4.39	2.26, 1.90	1.98[b]	3.57[b] (Hδ)
Lys^{270}	8.44	4.37	1.84, 1.76	1.45[b]	1.66[b] (Hδ), 2.99[b] (Hε)
Gly^{271}	8.34	3.93[b]			
Glu^{272}	8.19	4.46	2.15, 1.97	2.46[b]	
Thr^{273}	8.08	4.32	4.32	1.17	

[a] Measured at 500 MHz and 298 K in water containing 10% D_2O with H_2O (δ_H 4.76 ppm) as internal standard. The glycopeptide existed in two forms in solution due to *cis*/*trans* isomerization of the Gly^{268}−Pro^{269} amide bond. Shifts are reported for the major *trans*-isomer (displayed NOEs between Gly^{268} H$^{\alpha}$ and Pro^{269} H$^{\delta,\delta'}$), while the minor *cis*-isomer (<7%) could not be completely assigned due to spectral overlap. [b] Degeneracy has been assumed. [c] Chemical shifts for the galactose moiety: δ 4.42 (H1), 3.90 (H4), 3.75 (H6), 3.68 (H5), 3.63 (H3), and 3.51 (H2).

Table 7. ^{1}H NMR Chemical Shifts for CII259−273 with GalHyl^{264} and Ala$^{261}\psi$[(*Z*)-CH═CH]Gly^{262} (**34**)[a]

residue	NH	Hα	Hβ	Hγ	others
Gly^{259}		3.83[b]			
Ile^{260}	8.41	4.07	1.76	1.43, 1.13, 0.83 (CH_3)	0.82 (Hδ)
Ala$^{261}\psi$[(*Z*)-CH═CH]	8.30	4.58	1.16		5.47 and 5.44 (CH═CH)
Gly^{262}		3.11[b]			
Phe^{263}	8.11	4.58	3.08, 3.01		7.23 (Hδ), 7.32 (Hε), 7.30 (Hζ)
Hyl^{264}	8.41	4.28	2.00, 1.74	1.60[b]	4.04 (Hδ), 3.06 and 2.98 (Hε)[c]
Gly^{265}	7.91	3.90, 3.86			
Glu^{266}	8.21	4.37	2.10, 1.94	2.45[b]	
Gln^{267}	8.47	4.37	2.11, 1.97	2.36[b]	7.48 and 6.81 (δNH_2)
Gly^{268}	8.26	4.13, 3.98			
Pro^{269}		4.39	2.26, 1.90	1.98[b]	3.58[b] (Hδ)
Lys^{270}	8.44	4.29	1.83, 1.76	1.44[b]	1.67[b] (Hδ), 2.98[b] (Hε)
Gly^{271}	8.34	3.93[b]			
Glu^{272}	8.18	4.47	2.15, 1.98	2.48[b]	
Thr^{273}	8.16	4.38	4.34	1.17	

[a] Measured at 500 MHz and 298 K in water containing 10% D_2O with H_2O (δ_H 4.76 ppm) as internal standard. The glycopeptide existed in two forms in solution due to *cis*/*trans* isomerization of the Gly^{268}−Pro^{269} amide bond. Shifts are reported for the major *trans*-isomer (displayed NOEs between Gly^{268} H$^{\alpha}$ and Pro^{269} H$^{\delta,\delta'}$), while the minor *cis*-isomer (<11%) could not be completely assigned due to spectral overlap. [b] Degeneracy has been assumed. [c] Chemical shifts for the galactose moiety: δ 4.42 (H1), 3.91 (H4), 3.75 (H6), 3.68 (H5), 3.63 (H3), and 3.51 (H2).

attached to the solid phase (48 μmol) according to the general procedure described above, with the modification of coupling Ac-Ile-OH (4.0 equiv) at the N-terminal using HOBt (6 equiv) and DIC (3.9 equiv) as coupling reagents. Deacetylation was performed in several small scales (1.5−7 mg) by treatment with NaOMe in MeOH (5 mM, 1 mL/mg peptide) and the reaction time was limited to 10 min. The final purification using reversed-phase HPLC was performed twice, the second time using a 0−100% linear gradient of MeOH (0.1% TFA) in H_2O (0.1% TFA) over 40 min to afford **28** (3.8 mg, 7% yield based on the amount of resin used) as a white amorphous solid after lyophilization. MS (MALDI-TOF) calcd for $[M + Na]^+$, 1089.5; found, 1089.4. ^{1}H NMR data are given in Table 2.

Ac-L-isoleucyl-L-alanylψ[$CH_2NH_2^+$]glycyl-L-phenylalanyl-5-*O*-(β-D-galactopyranosyl)-5-hydroxy-L-lysylglycyl-L-glutam-1-yl-L-glutamine (29). Synthesis was performed with building block **2**

attached to the solid phase (48 μmol) according to the general procedure described above, with the modification of acetylating the N-terminal by treatment with Ac_2O/DMF (2:1) for 3 h. This afforded **29** (16 mg, 26% yield based on the amount of resin used) as a white amorphous solid after lyophilization. MS (MALDI-TOF) calcd 1054.5 $[M + H]^+$, found 1054.7. ^{1}H NMR data are given in Table 3.

Glycyl-L-isoleucyl-L-alanylψ[COCH$_2$]glycyl-L-phenylalanyl-5-*O*-(β-D-galactopyranosyl)-5-hydroxy-L-lysylglycyl-L-glutam-1-yl-L-glutaminylglycyl-L-prolyl-L-lysylglycyl-L-glutam-1-yl-L-threonine (31). Synthesis was performed with building block **1** attached to the solid phase (50 μmol) according to the general procedure described above, with the modification of coupling Boc-Gly-Ile-OH[85] (2.0 equiv) at the N-terminal using HATU (2.1 equiv) and 2,4,6-collidine (4.2 equiv) in CH_2Cl_2. This coupling was repeated using 1.0 equiv of Boc-Gly-Ile-OH. Deacetylation was performed in several small scales (0.5−8 mg) and the reaction time was limited to 10 min. The final purification using reversed-phase HPLC was performed twice, the second time using a 0−100% linear gradient of MeOH (0.1% TFA) in H_2O (0.1% TFA) over 40 min to afford **31** (7 mg, 7% yield based on the amount of resin used) as a white amorphous solid. MS (MALDI-TOF) calcd 1652.8 $[M + H]^+$, found 1652.8. ^{1}H NMR data are given in Table 4.

Glycyl-L-isoleucyl-L-alanylψ[CH$_2$NH$_2^+$]glycyl-L-phenylalanyl-5-*O*-(β-D-galactopyranosyl)-5-hydroxy-L-lysylglycyl-L-glutam-1-yl-L-glutaminylglycyl-L-prolyl-L-lysylglycyl-L-glutam-1-yl-L-threonine (32). Synthesis was performed with building block **2** attached to the solid phase (50 μmol) according to the general procedure described above. This afforded **32** (19.5 mg, 19% yield based on the amount of resin used) as a white amorphous solid after lyophilization. MS (MALDI-TOF) calcd 1639.8 $[M + H]^+$, found 1639.8. ^{1}H NMR data are given in Table 5.

Glycyl-L-isoleucyl-L-alanylψ[(*E*)-CH=CH]glycyl-L-phenylalanyl-5-*O*-(β-D-galactopyranosyl)-5-hydroxy-L-lysylglycyl-L-glutam-1-yl-L-glutaminylglycyl-L-prolyl-L-lysylglycyl-L-glutam-1-yl-L-threonine (33). Synthesis was performed with building block **3** attached to the solid phase (50 μmol) according to the general procedure described above. This afforded **33** (19 mg, 19% yield based on the amount of resin used) as a white amorphous solid after lyophilization. MS (MALDI-TOF) calcd 1636.8 $[M + H]^+$, found 1636.9. ^{1}H NMR data are given in Table 6.

Glycyl-L-isoleucyl-L-alanylψ[(*Z*)-CH=CH]glycyl-L-phenylalanyl-5-*O*-(β-D-galactopyranosyl)-5-hydroxy-L-lysylglycyl-L-glutam-1-yl-L-glutaminylglycyl-L-prolyl-L-lysylglycyl-L-glutam-1-yl-L-threonine (34). Synthesis was performed with building block **26** attached to the solid phase (50 μmol) according to the general procedure described above. This afforded **34** (22.6 mg, 23% yield based on the amount of resin used) as a white amorphous solid after lyophilization. MS (MALDI-TOF) calcd 1636.8 $[M + H]^+$, found 1636.8. ^{1}H NMR data are given in Table 7.

Inhibition Assay. The ability of the backbone-modified glycopeptides to bind to the A^q molecule was studied in an inhibition assay, performed essentially as described elsewhere.[17,42] Briefly, a 96-well microtiter plate was first coated with the mAb Y3-P (10 μg/mL) by incubating for 2 h at room temperature. Blocking was achieved by treatment with PBS containing 2% low fat milk for 1 h and this was followed by washing. Recombinant A^q proteins (0.1 μM) were then captured by incubating overnight at 4 °C. After washing, 100 μL of a mixture containing a fixed concentration of biotinylated CLIP peptide (2.5 μM) and increasing concentrations of the (modified) glycopeptides **27**−**34** (0 μM, 0.8 μM, 4 μM, 20 μM, 100 μM, and 500 μM) in 100 mM phosphate buffer (pH 7.0) was then incubated for 48 h at room temperature. This mixture also contained a cocktail of protease inhibitors (Complete, Boehringer, Mannheim). Excess of peptide was removed by washing with PBS, and the amount of biotinylated CLIP peptide bound to the recombinant A^q proteins was quantified using the dissociation-enhanced lanthanide fluoroimmunoassay (DELFIA) system based on the time-resolved fluoroimmunoassay technique with europium-labeled streptavidin (Wallac, Turku), according to the manufacturers instructions. All glycopeptides were evaluated on the same plate using biological material from the same batch. The experiments were performed in duplicates.

Determination of T-Cell Hybridoma Responses. The response of each glycopeptide-specific and A^q-restricted T-cell hybridoma line, that is, the amount of IL-2 secreted following incubation of the hybridoma with antigen-presenting spleen cells expressing A^q and increasing concentrations of the glycopeptides, was determined in a standard assay using ELISA. In brief, 5×10^4 T-cell hybridomas were co-cultured with 5×10^5 syngeneic spleen cells and increasing concentrations of the glycopeptides **27**−**34** (0 μM, 0.00128 μM, 0.0064 μM, 0.032 μM, 0.16 μM, 0.8 μM, 4 μM, and 20 μM) in a volume of 200 μL in 96-well flat-bottom microtiter plates. After 24 h, 100 μL aliquots of the supernatants were removed and frozen to kill any transferred T cells hybridoma. The contents of IL-2 in the culture supernatant were measured by sandwich ELISA (purified rat anti-mouse IL-2 as capturing mAb and the biotin rat anti-mouse IL-2 as detecting mAb, both from PharMingen, Los Angeles, CA) using the DELFIA system (Wallac, Turku, Finland). Recombinant mouse IL-2 served as a positive control and standard.

Acknowledgment. This work was funded by grants from the Swedish Research Council and the Biotechnology Fund at Umeå University. We are grateful to Drs. David Blomberg, Tomas Gustafsson, and Lotta Holm for helpful discussions, Dr. Mattias Hedenström for assistance with NMR spectroscopy, and David Andersson for providing docking scripts.

Note Added after ASAP Publication. This manuscript was released ASAP on October 18, 2007 with a typographical error in the Results and Discussion. The correct version posted on October 23, 2007.

Supporting Information Available: Coordinates of the comparative model of A^q, details of the molecular modeling, the modified experimental procedures for the galactosylated hydroxylysine derivative, purity of the glycopeptides, HPLC chromatograms for the backbone-modified glycopeptides, inhibition data for glycopeptide binding to A^q, T-cell response data with dose−response curves, and ^{1}H NMR and ^{13}C NMR spectra for all new isolated compounds. This material is available free of charge via the Internet at http://pubs.acs.org.

References

(1) Arnett, F. C.; Edworthy, S. M.; Bloch, D. A.; McShane, D. J.; Fries, J. F.; Cooper, N. S.; Healey, L. A.; Kaplan, S. R.; Liang, M. H.; Luthra, H. S.; Medsger, T. A. Jr.; Mitchell, D. M.; Neustadt, D. H.; Pinals, R. S.; Schaller, J. G.; Sharp, J. T.; Wilder, R. L.; Hunder, G. G. The American Rheumatism Association 1987 Revised Criteria for the Classification of Rheumatoid Arthritis. *Arthritis Rheum.* **1988**, *31*, 315−324.

(2) Astorga, G. P.; Williams, Jr, R. C. Altered Reactivity in Mixed Lymphocyte Culture of Lymphocytes from Patients with Rheumatoid Arthritis. *Arthritis Rheum.* **1969**, *12*, 547−554.

(3) Stastny, P. Mixed Lymphocyte Cultures in Rheumatoid Arthritis. *J. Clin. Invest.* **1976**, *57*, 1148−1157.

(4) Gregersen, P.; Silver, J.; Winchester, R. The Shared Epitope Hypothesis. An Approach to Understanding the Molecular Genetics of Susceptibility to Rheumatoid Arthritis. *Arthritis Rheum.* **1987**, *30*, 1205−1213.

(5) McFarland, B. J.; Beeson, C. Binding Interactions Between Peptides and Proteins of the Class II Major Histocompatibility Complex. *Med. Res. Rev.* **2002**, *22*, 168−203.

(6) Londei, M.; Savill, C. M.; Verhoef, A.; Brennan, F.; Leech, Z. A.; Duance, V.; Maini, R. N.; Feldmann, M. Persistence of Collagen Type II-Specific T-Cell Clones in the Synovial Membrane of a Patient with Rheumatoid Arthritis. *Proc. Natl. Acad. Sci. U.S.A.* **1989**, *86*, 636−640.

(7) Kim, H. Y.; Kim, W. U.; Cho, M. L.; Lee, S. K.; Youn, J.; Kim, S. I.; Yoo, W. H.; Park, J. H.; Min, J. K.; Lee, S. H.; Park, S. H.; Cho, C. S. Enhanced T Cell Proliferative Response to Type II Collagen and Synthetic Peptide CII (255−274) in Patients with Rheumatoid Arthritis. *Arthritis Rheum.* **1999**, *42*, 2085−2093.

(8) Bäcklund, J.; Carlsen, S.; Höger, T.; Holm, B.; Fugger, L.; Kihlberg, J.; Burkhardt, H.; Holmdahl, R. Predominant Selection of T Cells Specific for the Glycosylated Collagen Type II Epitope (263−270) in Humanized Transgenic Mice and in Rheumatoid Arthritis. *Proc. Natl. Acad. Sci. U.S.A.* **2002**, *99*, 9960−9965.
(9) Menzel, J.; Steffen, C.; Kolarz, G.; Eberl, R.; Frank, O.; Thumb, N. Demonstration of Antibodies to Collagen and of Collagen-Anticollagen Immune Complexes in Rheumatoid Arthritis Synovial Fluids. *Ann. Rheum. Dis.* **1976**, *35*, 446−450.
(10) Cook, A. D.; Stockman, A.; Brand, C. A.; Tait, B. D.; Mackay, I. R.; Muirden, K. D.; Bernard, C. C. A.; Rowley, M. J. Antibodies to Type II Collagen and HLA Disease Susceptibility Markers in Rheumatoid Arthritis. *Arthritis Rheum.* **1999**, *42*, 2569−2576.
(11) Burkhardt, H.; Koller, T.; Engström, Å.; Nandakumar, K. S.; Turnay, J.; Kraetsch, H. G.; Kalden, J. R.; Holmdahl, R. Epitope-Specific Recognition of Type II Collagen by Rheumatoid Arthritis Antibodies Is Shared With Recognition by Antibodies that are Arthritogenic in Collagen-Induced Arthritis in the Mouse. *Arthritis Rheum.* **2002**, *46*, 2339−2348.
(12) Courtenay, J. S.; Dallman, M. J.; Dayan, A. D.; Martin, A.; Mosedale, B. Immunisation Against Heterologous Type II Collagen Induces Arthritis in Mice. *Nature* **1980**, *283*, 666−668.
(13) Wooley, P. H.; Luthra, H. S.; Stuart, J. M.; David, C. S. Type II Collagen-Induced Arthritis in Mice. I. Major Histocompatibility Complex (I Region) Linkage and Antibody Correlates. *J. Exp. Med.* **1981**, *154*, 688−700.
(14) Brunsberg, U.; Gustafsson, K.; Jansson, L.; Michaëlsson, E.; Ährlund-Richter, L.; Pettersson, S.; Mattsson, R.; Holmdahl, R. Expression of a Transgenic Class II Ab Gene Confers Susceptibility to Collagen-Induced Arthritis. *Eur. J. Immunol.* **1994**, *24*, 1698−1702.
(15) Holm, B.; Bäcklund, J.; Recio, M. A. F.; Holmdahl, R.; Kihlberg, J. Glycopeptide Specificity of Helper T Cells Obtained in Mouse Models for Rheumatoid Arthritis. *ChemBioChem* **2002**, *3*, 1209−1222.
(16) Rosloniec, E. F.; Whittington, K. B.; Brand, D. D.; Myers, L. K.; Stuart, J. M. Identification of MHC Class II and TCR Binding Residues in the Type II Collagen Immunodominant Determinant Mediating Collagen-Induced Arthritis. *Cell. Immunol.* **1996**, *172*, 21−28.
(17) Kjellén, P.; Brunsberg, U.; Broddefalk, J.; Hansen, B.; Vestberg, M.; Ivarsson, I.; Engström, Å.; Svejgaard, A.; Kihlberg, J.; Fugger, L.; Holmdahl, R. The Structural Basis of MHC Control of Collagen-Induced Arthritis; Binding of the Immunodominant Type II Collagen 256−270 Glycopeptide to H-2A^q and H-2A^p Molecules. *Eur. J. Immunol.* **1998**, *28*, 755−767.
(18) Michaëlsson, E.; Broddefalk, J.; Engström, Å.; Kihlberg, J.; Holmdahl, R. Antigen Processing and Presentation of a Naturally Glycosylated Protein Elicits Major Histocompatibility Complex Class II-Restricted, Carbohydrate-Specific T Cells. *Eur. J. Immunol.* **1996**, *26*, 1906−1910.
(19) Broddefalk, J.; Bäcklund, J.; Almqvist, F.; Johansson, M.; Holmdahl, R.; Kihlberg, J. T Cells Recognize a Glycopeptide Derived from Type II Collagen in a Model for Rheumatoid Arthritis. *J. Am. Chem. Soc.* **1998**, *120*, 7676−7683.
(20) Corthay, A.; Bäcklund, J.; Broddefalk, J.; Michaëlsson, E.; Goldschmidt, T. J.; Kihlberg, J.; Holmdahl, R. Epitope Glycosylation Plays a Critical Role for T Cell Recognition of Type II Collagen in Collagen-Induced Arthritis. *Eur. J. Immunol.* **1998**, *28*, 2580−2590.
(21) Holm, B.; Baquer, S. M.; Holm, L.; Holmdahl, R.; Kihlberg, J. Role of the Galactosyl Moiety of Collagen Glycopeptides for T-Cell Stimulation in a Model for Rheumatoid Arthritis. *Bioorg. Med. Chem.* **2003**, *11*, 3981−3987.
(22) Wellner, E.; Gustafsson, T.; Bäcklund, J.; Holmdahl, R.; Kihlberg, J. Synthesis of a *C*-Glycoside Analogue of β-D-Galactosyl Hydroxynorvaline and its Use in Immunological Studies. *ChemBioChem* **2000**, *1*, 272−280.
(23) Marin, J.; Blaton, M. A.; Briand, J. P.; Chiocchia, G.; Fournier, C.; Guichard, G. Synthesis of Glycopeptides from Type II Collagen-Incorporating Galactosylated Hydroxylysine Mimetics and Their Use in Studying the Fine Specificity of Arthritogenic T Cells. *ChemBioChem* **2005**, *6*, 1796−1804.
(24) Gustafsson, T.; Hedenström, M.; Kihlberg, J. Synthesis of a *C*-Glycoside Analogue of β-D-Galactosyl Hydroxylysine and Incorporation in a Glycopeptide from Type II Collagen. *J. Org. Chem.* **2006**, *71*, 1911−1919.
(25) Holm, L.; Kjellén, P.; Holmdahl, R.; Kihlberg, J. Identification of the Minimal Glycopeptide Core Recognized by T Cells in a Model for Rheumatoid Arthritis. *Bioorg. Med. Chem.* **2005**, *13*, 473−482.
(26) Holm, L.; Frech, K.; Dzhambazov, B.; Holmdahl, R.; Kihlberg, J.; Linusson, A. Quantitative Structure-Activity Relationship of Peptides Binding to the Class II Major Histocompatibility Complex Molecule A^q Associated with Autoimmune Arthritis. *J. Med. Chem.* **2007**, *50*, 2049−2059.
(27) Dzhambazov, B.; Nandakumar, K. S.; Kihlberg, J.; Fugger, L.; Holmdahl, R.; Vestberg, M. Therapeutic Vaccination of Active Arthritis with a Glycosylated Collagen Type II Peptide in Complex with MHC Class II Molecules. *J. Immunol.* **2006**, *176*, 1525−1533.
(28) Bäcklund, J.; Treschow, A.; Bockermann, R.; Holm, B.; Holm, L.; Issazadeh-Navikas, S.; Kihlberg, J.; Holmdahl, R. Glycosylation of Type II Collagen is of Major Importance for T Cell Tolerance and Pathology in Collagen-Induced Arthritis. *Eur. J. Immunol.* **2002**, *32*, 3776−3784.
(29) Rosloniec, E. F.; Brandstetter, T.; Leyer, S.; Schwaiger, F. W.; Nagy, Z. A. Second-Generation Peptidomimetic Inhibitors of Antigen Presentation Effectively Treat Autoimmune Diseases in HLA-DR-Transgenic Mouse Models. *J. Autoimmunity* **2006**, *27*, 182−195.
(30) Sloan-Lancaster, J.; Allen, P. M. Altered Peptide Ligand-Induced Partial T Cell Activation. *Annu. Rev. Immunol.* **1996**, *14*, 1−27.
(31) Smilek, D. E.; Wraith, D. C.; Hodgkinson, S.; Dwivedy, S.; Steinman, L.; McDevitt, H. O. A Single Amino Acid Change in a Myelin Basic Protein Peptide Confers the Capacity to Prevent Rather Than Induce Experimental Autoimmune Encephalomyelitis. *Proc. Natl. Acad. Sci. U.S.A.* **1991**, *88*, 9633−9637.
(32) Gautam, A. M.; Lock, C. B.; Smilek, D. E.; Pearson, C. I.; Steinman, L.; McDevitt, H. O. Minimum Structural Requirements for Peptide Presentation by Major Histocompatibility Complex Class II Molecules: Implications in Induction of Autoimmunity. *Proc. Natl. Acad. Sci. U.S.A.* **1994**, *91*, 767−771.
(33) Hart, M.; Beeson, C. Utility of Azapeptides as Major Histocompatibility Complex Class II Protein Ligands for T-Cell Activation. *J. Med. Chem.* **2001**, *44*, 3700−3709.
(34) Bolin, D. R.; Swain, A. L.; Sarabu, R.; Berthel, S. J.; Gillespie, P.; Huby, N. J. S.; Makofske, R.; Orzechowski, L.; Perrotta, A.; Toth, K.; Cooper, J. P.; Jiang, N.; Falcioni, F.; Campbell, R.; Cox, D.; Gaizband, D.; Belunis, C. J.; Vidovic, D.; Ito, K.; Crowther, R.; Kammlott, U.; Zhang, X.; Palermo, R.; Weber, D.; Guenot, J.; Nagy, Z.; Olson, G. L. Peptide and Peptide Mimetic Inhibitors of Antigen Presentation by HLA-DR Class II MHC Molecules. Design, Structure−Activity Relationships, and X-ray Crystal Structures. *J. Med. Chem.* **2000**, *43*, 2135−2148.
(35) Mézière, C.; Viguier, M.; Dumortier, H.; Lo-Man, R.; Leclerc, C.; Guillet, J. G.; Briand, J. P.; Muller, S. In Vivo T Helper Cell Response to Retro-Inverso Peptidomimetics. *J. Immunol.* **1997**, *159*, 3230−3237.
(36) Cotton, J.; Hervé, M.; Pouvelle, S.; Maillère, B.; Ménez, A. Pseudopeptide Ligands for MHC II-Restricted T Cells. *Int. Immunol.* **1998**, *10*, 159−166.
(37) Ettouati, L.; Salvi, J. P.; Trescol-Biémont, M. C.; Walchshofer, N.; Gerlier, D.; Rabourdin-Combe, C.; Paris, J. Substitution of Peptide Bond 53−54 of HEL(52−61) with an Ethylene Bond Rather Than Reduced Peptide Bond is Tolerated by an MHC-II Restricted T Cell. *Pept. Res.* **1996**, *9*, 248−253.
(38) Ettouati, L.; Casimir, J. R.; Raynaud, I.; Trescol-Biémont, M. C.; Carrupt, P. A.; Gerlier, D.; Rabourdin-Combe, C.; Testa, B.; Paris, J. Synthesis, Biological Activity and Molecular Modelling of the 53−54 Ketomethylene Analogue of HEL(52−61). *Protein Pept. Lett.* **1998**, *5*, 221−229.
(39) Smith, A. B., III.; Benowitz, A. B.; Sprengeler, P. A.; Barbosa, J.; Guzman, M. C.; Hirschmann, R.; Schweiger, E. J.; Bolin, D. R.; Nagy, Z.; Campbell, R. M.; Cox, D. C.; Olson, G. L. Design and Synthesis of a Competent Pyrrolinone-Peptide Hybrid Ligand for the Class II Major Histocompatibility Complex Protein HLA-DR1. *J. Am. Chem. Soc.* **1999**, *121*, 9286−9298.
(40) Koehler, N. K. U.; Yang, C. Y.; Varady, J.; Lu, Y.; Wu, X.; Liu, M.; Yin, D.; Bartels, M.; Xu, B.; Roller, P. P.; Long, Y.; Li, P.; Kattah, M.; Cohn, M. L.; Moran, K.; Tilley, E.; Richert, J. R.; Wang, S. Structure-Based Discovery of Nonpeptidic Small Organic Compounds To Block the T Cell Response to Myelin Basic Protein. *J. Med. Chem.* **2004**, *47*, 4989−4997.
(41) Hedenström, M.; Holm, L.; Yuan, Z.; Emtenäs, H.; Kihlberg, J. Stereoselective Synthesis of Ψ[CH_2O] Pseudodipeptides and Conformational Analysis of a PheΨ[CH_2O]Ala Containing Analogue of the Drug Desmopressin. *Bioorg. Med. Chem. Lett.* **2002**, *12*, 841−844.
(42) Holm, L.; Bockermann, R.; Wellner, E.; Bäcklund, J.; Holmdahl, R.; Kihlberg, J. Side-Chain and Backbone Amide Bond Requirements for Glycopeptide Stimulation of T-Cells Obtained in a Mouse Model for Rheumatoid Arthritis. *Bioorg. Med. Chem.* **2006**, *14*, 5921−5932.
(43) Pietersz, G. A.; Pouniotis, D. S.; Apostolopoulos, V. Design of Peptide-Based Vaccines for Cancer. *Curr. Med. Chem.* **2006**, *13*, 1591−1607.
(44) Korber, B.; LaBute, M.; Yusim, K. Immunoinformatics Comes of Age. *PLoS Comput. Biol.* **2006**, *2*, e71.
(45) Davies, M. N.; Flower, D. R. Harnessing Bioinformatics to Discover New Vaccines. *Drug Discovery Today* **2007**, *12*, 389−395.

(46) *RCSB Protein Data Bank*; http://www.rcsb.org/pdb/home/home.do (accessed September 18, 2006).
(47) Zhu, Y.; Rudensky, A. Y.; Corper, A. L.; Teyton, L.; Wilson, I. A. Crystal Structure of MHC Class II I-A^b in Complex with a Human Clip Peptide: Prediction of an I-A^b Peptide-Binding Motif. *J. Mol. Biol.* **2003**, *326*, 1157−1174.
(48) Scott, C. A.; Peterson, P. A.; Teyton, L.; Wilson, I. A. Crystal Structures of Two I-A^d-Peptide Complexes Reveal That High Affinity Can Be Achieved without Large Anchor Residues. *Immunity* **1998**, *8*, 319−329.
(49) Liu, X.; Dai, S.; Crawford, F.; Frugé, R.; Marrack, P.; Kappler, J. Alternate Interactions Define the Binding of Peptides to the MHC Molecule IA^b. *Proc. Natl. Acad. Sci. U.S.A.* **2002**, *99*, 8820−8825.
(50) Déziel, R.; Plante, R.; Caron, V.; Grenier, L.; Llinas-Brunet, M.; Duceppe, J. S.; Malenfant, E.; Moss, N. A Practical and Diastereoselective Synthesis of Ketomethylene Dipeptide Isosteres of the Type AAΨ[$COCH_2$]Asp. *J. Org. Chem.* **1996**, *61*, 2901−2903.
(51) Våbenø, J.; Brisander, M.; Lejon, T.; Luthman, K. Diastereoselective Reduction of a Chiral *N*-Boc-Protected *δ*-Amino-α,*β*-unsaturated *γ*-Keto Ester Phe-Gly Dipeptidomimetic. *J. Org. Chem.* **2002**, *67*, 9186−9191.
(52) Blanchette, M. A.; Choy, W.; Davis, J. T.; Essenfeld, A. P.; Masamune, S.; Roush, W. R.; Sakai, T. Horner-Wadsworth-Emmons Reaction: Use of Lithium Chloride and an Amine for Base-Sensitive Compounds. *Tetrahedron Lett.* **1984**, *25*, 2183−2186.
(53) Våbenø, J.; Lejon, T.; Uhd Nielsen, C.; Steffansen, B.; Chen, W.; Ouyang, H.; Borchardt, R. T.; Luthman, K. Phe-Gly Dipeptidomimetics Designed for the Di-/Tripeptide Transporters PEPT1 and PEPT2: Synthesis and Biological Investigations. *J. Med. Chem.* **2004**, *47*, 1060−1069.
(54) Dale, J. A.; Dull, D. L.; Mosher, H. S. α-Methoxy-α-trifluoromethylphenylacetic Acid, a Versatile Reagent for the Determination of Enantiomeric Composition of Alcohols and Amines. *J. Org. Chem.* **1969**, *34*, 2543−2549.
(55) Boeijen, A.; van Ameijde, J.; Liskamp, R. M. J. Solid-Phase Synthesis of Oligourea Peptidomimetics Employing the Fmoc Protection Strategy. *J. Org. Chem.* **2001**, *66*, 8454−8462.
(56) Kokotos, G. A Convenient One-Pot Conversion of N-Protected Amino-Acids and Peptides into Alcohols. *Synthesis* **1990**, *4*, 299−301.
(57) Dess, D. B.; Martin, J. C. Readily Accessible 12-I-5 Oxidant for the Conversion of Primary and Secondary Alcohols to Aldehydes and Ketones. *J. Org. Chem.* **1983**, *48*, 4155−4156.
(58) Lubell, W. D.; Rapoport, H. Configurational Stability of N-Protected α-Amino Aldehydes. *J. Am. Chem. Soc.* **1987**, *109*, 236−239.
(59) Myers, A. G.; Zhong, B.; Movassaghi, M.; Kung, D. W.; Lanman, B. A.; Kwon, S. Synthesis of Highly Epimerizable *N*-protected α-Amino Aldehydes of High Enantiomeric Excess. *Tetrahedron Lett.* **2000**, *41*, 1359−1362.
(60) Abdel-Magid, A. F.; Carson, K. G.; Harris, B. D.; Maryanoff, C. A.; Shah, R. D. Reductive Amination of Aldehydes and Ketones with Sodium Triacetoxyborohydride. Studies on Direct and Indirect Reductive Amination Procedures. *J. Org. Chem.* **1996**, *61*, 3849−3862.
(61) Wiktelius, D.; Luthman, K. Taking Control of P1, P1′ and Double Bond Stereochemistry in the Synthesis of Phe-Phe (*E*)-Alkene Amide Isostere Dipeptidomimetics. *Org. Biomol. Chem.* **2007**, *5*, 603−605.
(62) McDougal, P. G.; Rico, J. G.; Oh, Y. I.; Condon, B. D. A Convenient Procedure for the Monosilylation of Symmetric 1,*n*-Diols. *J. Org. Chem.* **1986**, *51*, 3388−3390.
(63) Harnden, M. R.; Jarvest, R. L. Analogues of the Antiviral Acyclonucleoside 9-(4-Hydroxy-3-hydroxymethylbutyl)guanine. Part 4. Substitution on the 2-Amino Group. *J. Chem. Soc., Perkin Trans. I* **1989**, *12*, 2207−2213.
(64) Barry, C. S.; Bushby, N.; Harding, J. R.; Willis, C. L. Stereoselective Synthesis of the Tetrahydropyran Core of Polycarvernoside A. *Org. Lett.* **2005**, *7*, 2683−2686.
(65) Andersson, E. C.; Hansen, B. E.; Jacobsen, H.; Madsen, L. S.; Andersen, C. B.; Engberg, J.; Rothbard, J. B.; Sønderstrup McDevitt, G.; Malmström, V.; Holmdahl, R.; Svejgaard, A.; Fugger, L. Definition of MHC and T Cell Receptor Contacts in the HLA-DR4-Restricted Immunodominant Epitope in Type II Collagen and Characterization of Collagen-Induced Arthritis in HLA-DR4 and Human CD4 Transgenic Mice. *Proc. Natl. Acad. Sci. U.S.A.* **1998**, *95*, 7574−7579.
(66) Syed, B. M.; Gustafsson, T.; Kihlberg, J. 9-BBN as a Convenient Protecting Group in Functionalisation of Hydroxylysine. *Tetrahedron* **2004**, *60*, 5571−5575.
(67) González-Muñiz, R.; García-López, M. T.; Gómez-Monterrey, I.; Herranz, R.; Jimeno, M. L.; Suárez-Gea, M. L.; Johansen, N. L.; Madsen, K.; Thøgersen, H.; Suzdak, P. Ketomethylene and (Cyanomethylene)amino Pseudopeptide Analogues of the C-Terminal Hexapeptide of Neurotensin. *J. Med. Chem.* **1995**, *38*, 1015−1021.
(68) The deacetylation of **28** and **31** was initially performed in a small test scale and was allowed to proceed for a longer period of time (2 h) with careful monitoring by analytical reversed-phase HPLC. It was found that the deacetylation was complete after approximately 10 min, displaying one major product peak corresponding to the desired glycopeptide and one smaller peak with a slightly different retention time. With increasing reaction time, the ratio between the two peaks approached, and finally reached, 1:1. After separation, both peaks were found to have the correct mass when analyzed with LCMS, indicating that a mixture of diastereomers resulting from racemization of the stereocenter in the isostere had been obtained.
(69) McFarland, B. J.; Katz, J. F.; Sant, A. J.; Beeson, C. Energetics and Cooperativity of the Hydrogen Bonding and Anchor Interactions that Bind Peptides to MHC Class II Protein. *J. Mol. Biol.* **2005**, *350*, 170−183.
(70) Jensen, T.; Nielsen, M.; Gad, M.; Hansen, P.; Komba, S.; Meldal, M.; Ødum, N.; Werdelin, O. Radically Altered T Cell Receptor Signaling in Glycopeptide-Specific T Cell Hybridoma Induced by Antigen with Minimal Differences in the Glycan Group. *Eur. J. Immunol.* **2001**, *31*, 3197−3206.
(71) Matsui, K.; Boniface, J. J.; Steffner, P.; Reay, P. A.; Davis, M. M. Kinetics of T-Cell Receptor Binding to Peptide/I-E^k Complexes: Correlation of the Dissociation Rate with T-Cell Reponsiveness. *Proc. Natl. Acad. Sci. U.S.A.* **1994**, *91*, 12862−12866.
(72) Lyons, D. S.; Lieberman, S. A.; Hampl, J.; Boniface, J. J.; Chien, Y.; Berg, L. J.; Davis, M. M. A TCR Binds to Antagonist Ligands with Lower Affinities and Faster Dissociation Rates Than to Agonists. *Immunity* **1996**, *5*, 53−61.
(73) Kersh, G. J.; Kersh, E. N.; Fremont, D. H.; Allen, P. M. High- and Low-Potency Ligands with Similar Affinities for the TCR: The Importance of Kinetics in TCR Signaling. *Immunity* **1998**, *9*, 817−826.
(74) *Molecular Operating Environment (MOE)*, version 2005.06; Chemical Computing Group Inc.: 1010 Sherbrooke St. West Suite, 910 Montreal, Canada H3A 2R7.
(75) *Swiss-Prot/TREMBL*; http://www.expasy.org/sprot/ (accessed September 18, 2006).
(76) *Protein-protein BLAST*; http://www.ncbi.nlm.nih.gov/BLAST/ (accessed September 18, 2006).
(77) Word, J. M.; Lovell, S. C.; Richardson, J. S.; Richardson, D. C. Asparagine and Glutamine: Using Hydrogen Atom Contacts in the Choice of Side-Chain Amide Orientation. *J. Mol. Biol.* **1999**, *285*, 1735−1747.
(78) *BABEL*, version 1.6; OpenEye Scientific Software Inc.: 3600 Cerrillos Road, Suite 1107, Santa Fe, NM 87507.
(79) Weininger, D. SMILES, a Chemical Language and Information-System. 1. Introduction to Methodology and Encoding Rules. *J. Chem. Inf. Comput. Sci.* **1988**, *28*, 31−36.
(80) *CORINA*; Molecular Networks GmbH, Nägelsbachstra*β*e 25, 91052 Erlangen, Germany, http://www2.chemie.uni-erlangen.de/software/corina/free_struct.html (accessed November 1, 2006).
(81) *OMEGA*, version 2.0; OpenEye Scientific Software Inc.: 3600 Cerrillos Road, Suite 1107, Santa Fe, NM 87507.
(82) *FRED*, version 2.0.1; OpenEye Scientific Software Inc.: 3600 Cerrillos Road, Suite 1107, Santa Fe, NM 87507.
(83) Andersson, C. D.; Thysell, E.; Lindström, A.; Bylesjö, M.; Raubacher, F.; Linusson, A. A Multivariate Approach to Investigate Docking Parameters' Effects on Docking Performance. *J. Chem. Inf. Model.* **2007**, *47*, 1673−1687.
(84) Kofron, W. G.; Baclawski, L. M. A Convenient Method for Estimation of Alkyllithium Concentrations. *J. Org. Chem.* **1976**, *41*, 1879−1880.
(85) Bodanszky, M.; Bodanszky, A. Protecting Groups. In *The Practice of Peptide Synthesis*, 1st ed.; Hafner, K., Rees, C. W., Trost, B. M., Lehn, J. M., von Ragué Schleyer, P., Zahradník, R., Eds.; Springer-Verlag: New York, 1984; Vol. 21, pp 20.
(86) Brook, M. A.; Chan, T. H. A Simple Procedure for the Esterification of Carboxylic Acids. *Synthesis* **1983**, *3*, 201−203.
(87) Krchnak, V.; Vagner, J.; Lebl, M. Noninvasive Continous Monitoring of Solid-Phase Peptide Synthesis by Acid-Base Indicator. *Int. J. Pept. Prot. Res.* **1988**, *32*, 415−416.
(88) Kaiser, E.; Colescott, R. L.; Bossinger, C. D.; Cook, P. I. Color Test for Detection of Free Terminal Amino Groups in the Solid-Phase Synthesis of Peptides. *Anal. Biochem.* **1970**, *34*, 595−598.

JM0705410